Technical Note	1976-10
Simulation of a Narrow Bandpass-Limited Satellite Channel	B. E. White 28 July 1976

Lincoln Laboratory

MASSACHUSETTS INSTITUTE OF TECHNOLOGY

LEXINGTON, MASSACHUSETTS
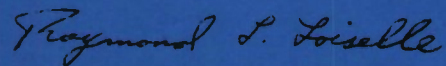
ADA030411

This technical report has been reviewed and is approved for publication.

FOR THE COMMANDER

Raymond L. Loiselle

Raymond L. Loiselle, Lt. Col., USAF
Chief, ESD Lincoln Laboratory Project Office

MASSACHUSETTS INSTITUTE OF TECHNOLOGY

LINCOLN LABORATORY

SIMULATION OF A NARROW
BANDPASS-LIMITED SATELLITE CHANNEL

B. E. WHITE

Group 67

TECHNICAL NOTE 1976-10

28 JULY 1976

LEXINGTON   MASSACHUSETTS

ABSTRACT

The effects of a bandpass-limiting satellite channel, such as a B=25-kHz hard-limiting FLEETSAT channel, on several modulation techniques were simulated The modulations included BPSK and various forms of QPSK, including offset QPSK and continuous-phase minimum frequency shift keying (MSK). Coherent matched-filter receivers and both uplink and downlink noise were assumed.

For a bit error probability of 0.005 and a SNR loss of less than 1 dB caused by the nonlinearity in the FLEETSAT case, the maximum standard data rate R was 19.2 kbps for BPSK but 32 kbps for offset QPSK, MSK and QPSK. Rates of 24 kbps for BPSK and 48 kbps for offset QPSK and MSK were attainable at this same reliability with a SNR degradation of about 4 dB and 2.5 dB, respectively. Larger degradations are expected at lower error rates.

TABLE OF CONTENTS

I.   INTRODUCTION AND SUMMARY

In this section we review the motivation for this study and present the principal results of our simulations. The simulation model is discussed in Section II, and the performance is analyzed in Section III.

1.1 Background

The next generation of military communications satellites denoted here by FLEETSAT's will have a number of 25-kHz[†] wide, bandpass hard-limiting channels at VHF/UHF frequencies [1]. When contemplating the most effective use of these resources, one of the issues that arises is the maximum data rate[*] feasible through each channel for a given modulation scheme. This issue is addressed here for coherent matched-filter receivers and modulation schemes employing various forms of antipodal signaling. The major modulations are: binary phase shift keying (BPSK), offset or staggered quadriphase shift keying (SQPSK), and minimum shift keying (MSK), a form of continuous-phase binary frequency shift keying (CPBFSK). The main objectives are to determine the better modulation techniques and to estimate performance losses with respect to a linear wideband channel as a function of data rate. The important issue of how the distortion introduced by the narrowband channel affects the synchronization techniques used with each modulation scheme for acquiring and tracking both symbol timing and phase or frequency offsets will not be treated here.

We model the satellite as a narrowband filter followed by an ideal bandpass limiter that removes the envelope modulation of its input (see Fig. 1.1). Since

---

[*]   Preferably selected from the standard families 75×2^n bps, n = 0, 1, 2,..., and $8000 \times N$ bps, N = 1, 2, 3,.... .

[†]   FLEETSAT's will also have 5-kHz channels and a 500-kHz channel; the results of this report apply to these channels with appropriate bandwidth normalization.

TRANSMITTER   SATELLITE   RECEIVER

```
┌──────────────┐        ┌──────────────┐  ┌──────────────┐        ┌──────────────┐
│              │        │   FILTER     │  │    IDEAL     │        │   COHERENT   │
│  MODULATOR   │──→ (+) →│ (B = 3-dB    │→ │  BANDPASS    │→ (+) →│   MATCHED    │
│              │    ↑    │  bandwidth)  │  │   LIMITER    │   ↑    │    FILTER    │
└──────────────┘    │    └──────────────┘  └──────────────┘   │    └──────────────┘
                    │                                         │
              ┌──────────┐                              ┌──────────┐
              │  UPLINK  │                              │ DOWNLINK │
              │  NOISE   │                              │  NOISE   │
              └──────────┘                              └──────────┘        18-6-17038-1
```
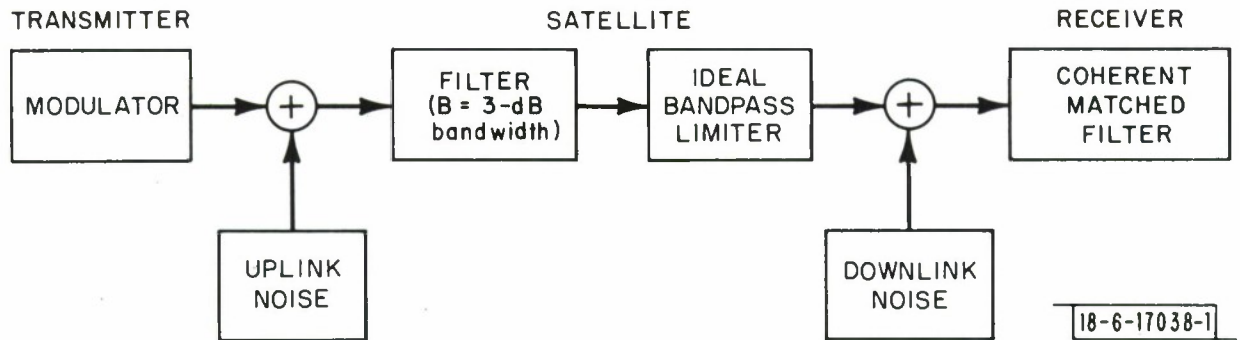
Fig. 1.1.   Computer simulation model.

2

the space segment of the system is well past the design stage, we view the satellite as fixed and have concentrated our effort in this area on developing a reasonable model of a satellite filter from data made available to us through the Navy.

Typical characteristics of a FLEETSAT filter are shown in Fig. 1.2. The filtering is actually done by a cascade of two filters denoted by A and B with a combined 3-dB bandwidth closer to 27 kHz than 25 kHz. The actual center frequency of this filter may vary by ± 1 kHz according to the FLEETSAT satellite specification. In this report we normalized bandwidths and data rates to a 3-dB filter bandwidth of 25 kHz to be slightly conservative.

The phase deviation curve of Fig. 1.2b covers most of the filter's 3-dB bandwidth. The FLEETSAT specifcation called for near linearity over the center 80% of the useful bandwidth. The linear-phase reference evidently resulted from a best-fit straight line through the band center. A slightly smaller slope tangent to the phase characteristic at the zero frequency deviation would result in a phase deviation of about 30 degrees at 10 kHz and -6 degrees at -10 kHz.

We have simulated several filters to obtain information on system performance sensitivity to a difference in spectral roll-off, phase nonlinearity and center frequency offset. This might suggest new specification criteria in the future.

Although the space segment is considered inaccessible, we may well have the freedom to modify communication terminals belonging to the earth segment.

3
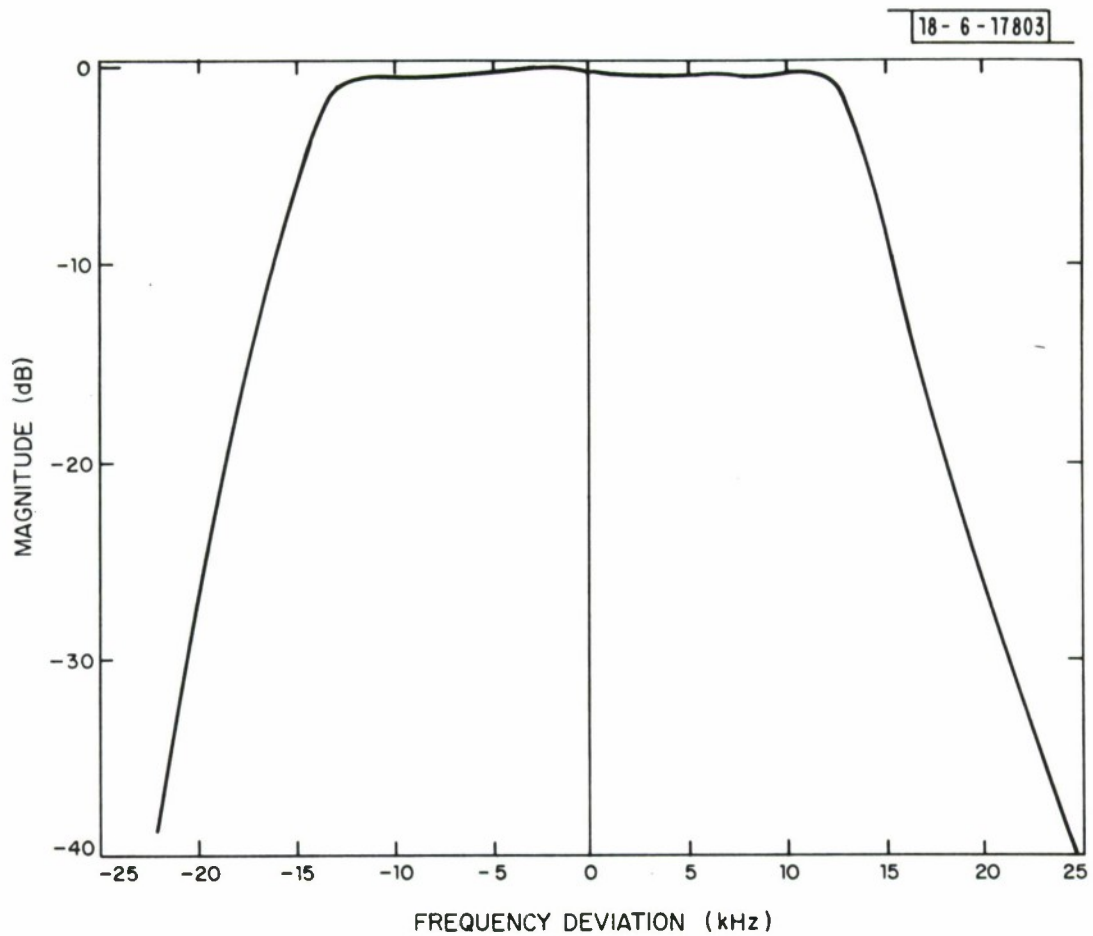
a. Response of filter A (filter B's response is similar).

Fig. 1.2. Typical characteristics of a FLEETSAT channel filter.

18- 6- 17804
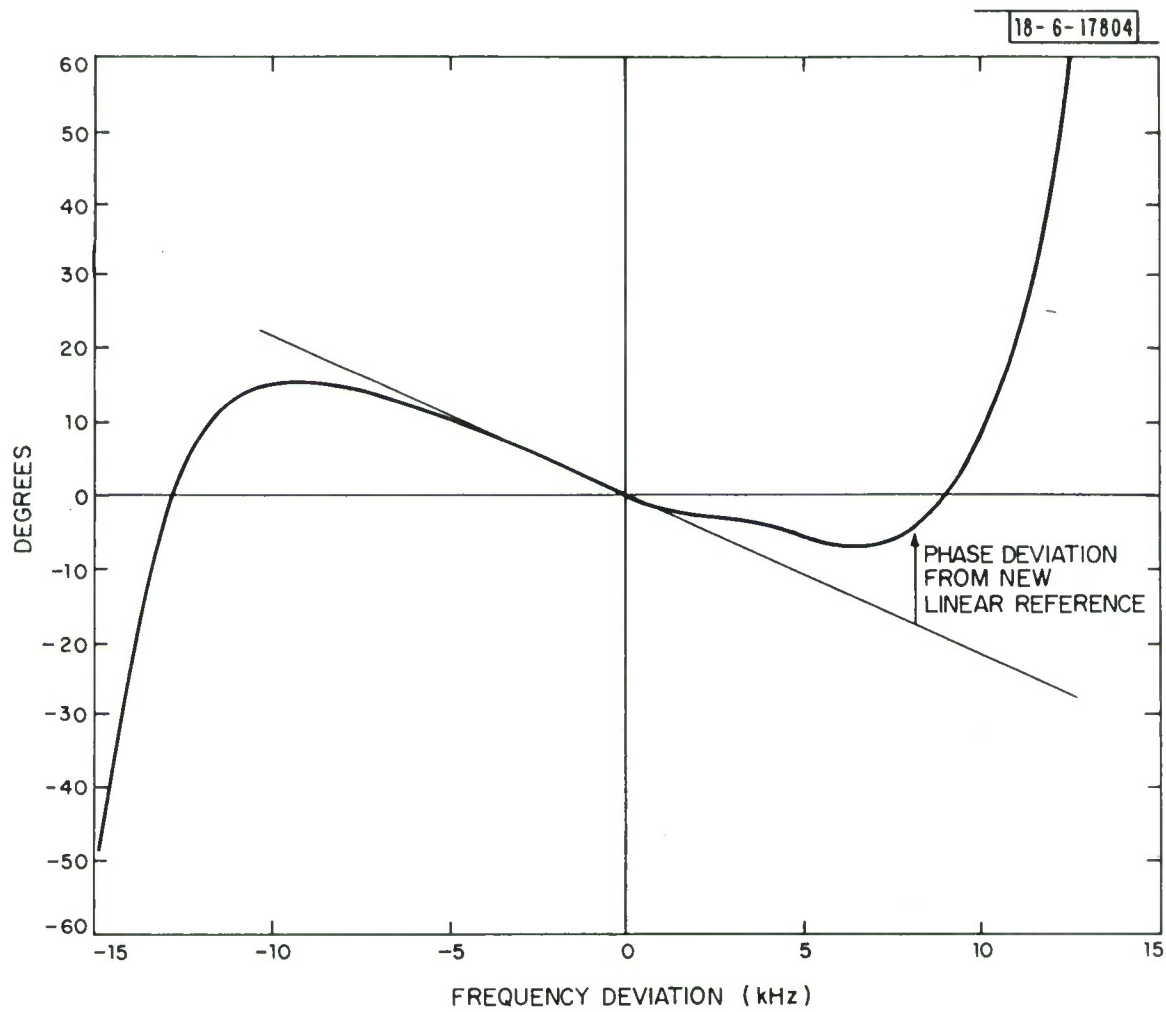
b. Phase deviation relative to linear reference.
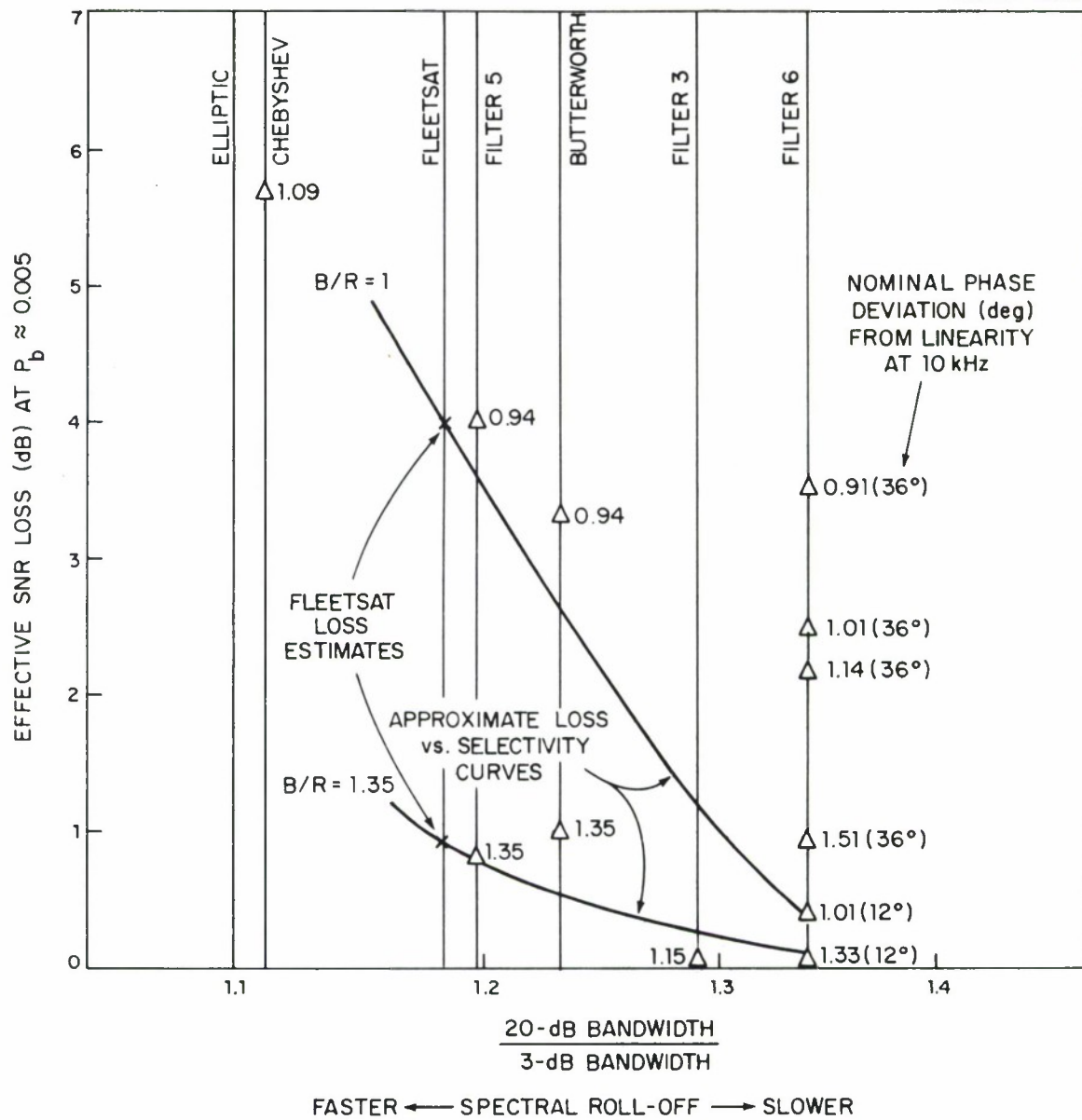
Fig. 1.2. Continued.

This is the principal reason for considering modulation techniques in addition to the more common BPSK used with the WSC-3 modem [2], for example. A next step would be to investigate sophisticated (possibly adaptive) receiver structures that are better matched to the distorted waveforms transmitted by the nonlinear narrowband satellite.

1.2 Conclusions

Six modulation techniques that yield equivalent coherent, matched-filter performance in the presence of additive white Gaussian noise (AWGN) were simulated for the narrow bandpass-limited satellite model. Of these modulation techniques, BPSK performed far worse than the others at the same data rates. MSK and SQPSK proved to be the best modulations overall, followed closely by quadriphase shift keying (QPSK), and more distantly by a modulation scheme we call alternating QPSK (AQPSK) and a form of continuous-phase quadrifrequency shift keying (CPQFSK) (see Section 2.2.). In this section we shall focus mainly on the best modulations MSK and SQPSK because they are so attractive, and the worst modulation scheme BPSK because it is so common.

The effective SNR losses for equal uplink and downlink SNR's compared to an AWGN channel at a bit error probability of $P_b \approx 0.005$ are depicted in Fig. 1.3 for BPSK and MSK. SQPSK performance is not significantly different from the MSK results of Fig. 1.3b. The data represent most of the simulations performed for these modulations using different satellite filter models.

The number beside each datum gives the ratio of the filter 3-dB bandwidth B and the data rate R for that simulation. The numbers in parenthesis for filter 6 in Fig. 1.3 refer to phase deviations defined below. The solid curves

a. BPSK.

Fig. 1.3. Performance loss vs. filter bandwidth ratio for various 3-dB bandwidth to data rate (B/R) ratios (equal uplink and downlink SNR's).
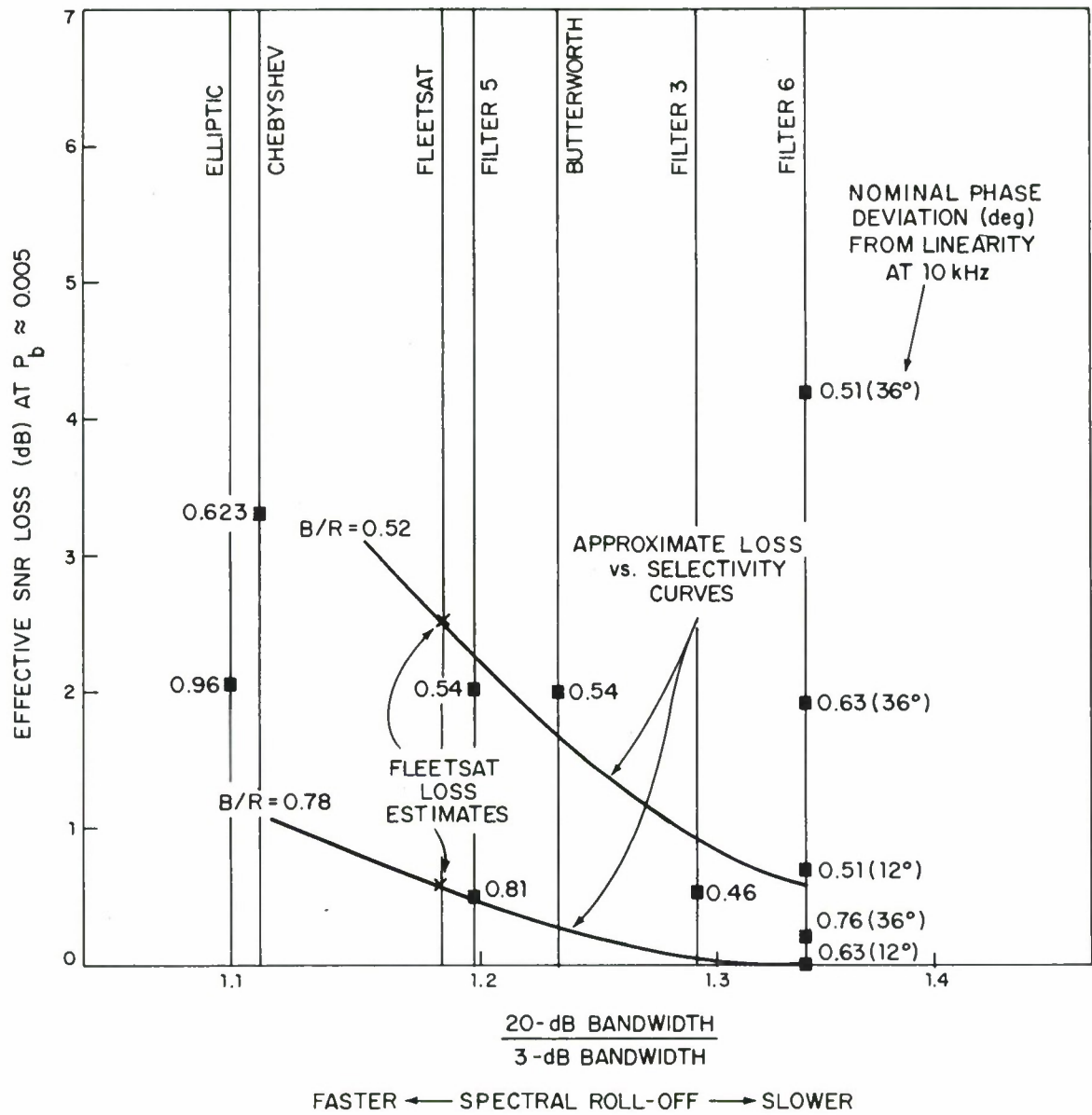
b. MSK.

Fig. 1.3. Continued.

are rather tenuous estimates of performance loss versus filter selectivity for constant B/R ratios. The X's mark the best FLEETSAT loss estimates. Although these estimates are not very sensitive to small changes in P_b, the losses would increase markedly with a decade or more decrease in P_b.

The performance degradations are plotted as a function of the ratio of the filter 20-dB and 3-dB bandwidths. In each part of Fig. 1.3, six labeled vertical lines mark these ratios for the filters simulated, while the seventh vertical line labeled FLEETSAT denotes the bandwidth ratio for the cascaded filter of Fig. 1.2, our current information as to the satellite filter characteristics.

This measure of spectral roll-off for a filter, the 20-dB to 3-dB bandwidth ratio, is also used in [3]. This ratio happens to vary from -7% to +13% for the filters simulated, relative to the FLEETSAT filter. The purpose of presenting the data in this form is to show how the performance loss depends on filter selectivity, defined as the above bandwidth ratio in this instance. This enables us to obtain a more accurate estimate of the true degradation for the FLEETSAT filter, once differences in phase non-linearities are taken into account.

Two versions of filter 6 (see Fig. 1.3) were employed, one with a nominal phase deviation of 12 degrees at 10 kHz, and the other with a deviation of 36 degrees. From the elliptic, Chebyshev and Butterworth phase characteristics in Appendix B, it can be verified that the Butterworth and Chebyshev phase deviations are roughly comparable in magnitude to the 12-degree and 36-degree deviations of filter 6, respectively; the elliptic phase deviation is an

order of magnitude larger.

On intuitive grounds and from the data of Fig. 1.3, we claim that the larger the bandwidth ratio, the more sensitive the performance loss is to a change in phase nonlinearity. This is because the magnitude characteristic dominates the nonlinear phase effects in regions of large attenuation. Thus, since the 12-degree filter 6 more closely approximates the known phase deviation for the FLEETSAT filter, more weight should be given to the 12-degree data than the 36-degree filter-6 data.

In drawing the curves of Fig. 1.3, then, the data for filter 5, the Butterworth filter and the 12-degree filter 6 were weighted more heavily, followed by the Chebyshev and 36-degree filter-6 data. The filter-3 data were given less emphasis because the phase characteristic is linear. On the other hand, the phase of the elliptic filter is too nonlinear. The intersections of the degradation curves with the FLEETSAT lines of Figs. 1.3a and b indicate our estimates of the performance losses to be anticipated for the poorest modulation scheme BPSK and the best modulations MSK and SQPSK.

In summary, we have the following major results for the simulation of the narrow bandpass-limited satellite channel:

A.   The best modulations studied are MSK and SQPSK. At a bit error probability of ≈ 0.005 a performance loss of less than 1 dB and 3 dB can be expected for data rates up to 32 kbps and 48 kbps, respectively, through a 25-kHz 3-dB bandwidth FLEETSAT channel, if either modulation scheme is employed with a coherent matched-filter receiver.

B.   The next best modulations are QPSK and AQPSK. QPSK often per-
forms as well as MSK or SQPSK, and any additional SNR loss for QPSK is gen-
erally less than 1 dB. AQPSK performs significantly worse than MSK, SQPSK
and QPSK at the larger data rates, but can still yield tolerable losses at
reduced rates.

C.   CPQFSK and BPSK are the worst modulations studied. Although
CPQFSK does much better than BPSK, neither modulation scheme is competitive
with the others at the larger data rates.

D.   BPSK would suffer a performance loss of no more than 1 dB at a
data rate of 19.2 kbps for a bit error probability of $\approx$ 0.005 and a 25-kHz
3-dB bandwidth FLEETSAT channel, but a loss of about 4 dB at a 24 kbps rate.

E.   For a reliability level of $\approx$ 0.005 bit error probability and a
performance loss of 1 dB or less, the maximum standard data rate possible
through a 25-kHz 3-dB bandwidth FLEETSAT channel is 19.2 kbps for BPSK,
24 kbps for AQPSK and CPQFSK, and 32 kbps for MSK, SQPSK and QPSK.

F.   BPSK is less sensitive to an offset in the center frequency of
the FLEETSAT channel than MSK or SQPSK. (See Fig. 3.4.)

These conclusions are generally either consistent with or corroborated by
other simulated or experimental results obtained independently [3-12]. But a
direct comparison of our data with that of the literature would be tenuous
because of significant differences in the various approaches. Furthermore,
such a comparison would be too lengthy for inclusion in this report.

Error rates as large as 10^{-2} are of interest in coded systems whereas
bit error probabilities of 10^{-3} and smaller are of interest in uncoded systems.

With narrow bandpass-limiting operation we expect larger degradations at the lower error rates since there the limitations are more likely to be filter selectivity and intermodulation effects rather than channel noise. Very little data were gathered below 10^{-3} because of the length of the simulations required with both uplink and downlink noise. Techniques exist for reducing the simulation time when the uplink noise is negligible [3,6].

II. SIMULATION MODEL

The bandlimited channel and modulations used in the computer simulation model are discussed in this section.

2.1 Channel Model

A block diagram of the simulation model was shown in Fig. 1.1. The UHF satellite model consists of a narrow bandpass filter of nominal 3-dB bandwidth B = 25 kHz followed by an ideal bandpass limiter which removes the envelope modulation of its input. Additive white Gaussian noise (AWGN) is assumed for both the uplink to the satellite and the downlink from the satellite. The entire simulation is performed digitally and at baseband with complex signals and noise. The coherent performance of techniques employing various forms of antipodal signaling and detection filters matched to the transmitted signals, and operating at the same data rate R will be compared on a common basis.

Data rates in excess of the filter bandwidth (B/R < 1) will be of principal interest. Thus, the relatively narrowband filter (generally with a nonlinear phase characteristic) and the highly nonlinear limiter will tend to constrain the signal spectrum and distort the received waveform thereby introducing a significant amount of intersymbol interference (ISI). Such ISI will be the principal source of degradation from the theoretical matched-filter performance in the presence of AWGN. For moderate uplink and downlink energy contrast ratios of interest $(E_b/N_o)_{up}$ and $(E_b/N_o)_{down}$, respectively, the limiter generally has a mitigating effect on the ISI. That is, compared to a linear transponder with the same average power, the hard-limiting operation can actually improve overall performance in some cases.

13

2.1.1 Matched-Filter Receiver

The uplink E_b/N_o is defined in the usual way as the ratio of the useful signal energy per data bit E_b received at the satellite to the single-sided uplink noise power spectral density N_o [13]. The downlink E_b/N_o is defined similarly assuming that all the satellite transmitter power is applied to a useful downlink signal. Of course, some of this downlink power is devoted to ISI produced by the narrow bandpass-limited channel and to repeating uplink noise. Hence, not all the downlink signal energy is really useful for detection, especially with a receiver matched to the undistorted uplink signals.

It has been recently demonstrated by computer simulation [14] that a 1 or 2 dB improvement in performance is possible with a more complex receiver structure. In this approach the matched filters are replaced by a set of crosscorrelators operating over an interval spanning most of the ISI. The reference signals are generated by passing a finite set of transmitted waveforms through an equivalent of the known channel in the absence of noise. This procedure approximates maximum-likelihood detection but is feasible only when the channel is known and time-invariant, and when most of the ISI is confined to a few signaling intervals.

The maximum-likelihood approach using the Viterbi algorithm is also an interesting possibility [15]. A preliminary investigation for BPSK indicates that nearly all the residual ISI could be removed with a digital processor of modest complexity [15a].

Thus, under certain conditions it is feasible to improve on the (mis) matched-filter performance. But for the purpose of this report we simply recognize this possibility and simulate only the matched-filter model. More sophisticated receivers will be left for future study.

2.1.2 Ideal Bandpass Limiter

Since the bandpass limiter can be implemented with a solid-state device at UHF with much less severe AM to PM conversion problems that can plague TWT implementations at GHz frequencies [4, 5, 16], the ideal (hard-limiting) bandpass-limiting model is reasonable for our simulation.

The ideal bandpass-limiting operation is depicted in Fig. 2.1 for a baseband complex input sample $x(n) + jy(n)$, marked by a clear dot in quadrant I. The limiter maps this point to the circle of radius r along a radial from the origin to yield a complex output sample $x'(n) + jy'(n)$, marked by a solid dot, where

$$x'(n) = \frac{rx(n)}{\sqrt{x^2(n) + y^2(n)}} \tag{2.1a}$$

$$y'(n) = \frac{ry(n)}{\sqrt{x^2(n) + y^2(n)}} . \tag{2.1b}$$

Hence, the limiter removes the amplitude modulation but preserves the phase information, i.e., for a narrowband, analog, bandpass input $V(t)\cos(\omega_c t + \phi(t))$ at a carrier frequency $\omega_c/2\pi$, the ideal bandpass-
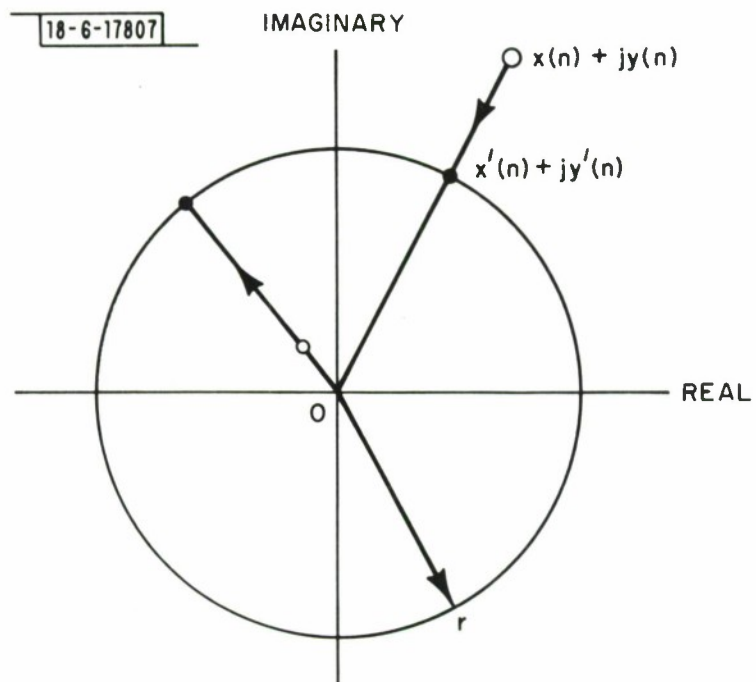
Fig. 2.1.   Ideal bandpass-limiting operation.

limiter output is $\cos(\omega_c t + \phi(t))$. From (2.1) we note that a change in either input generally produces crosstalk between the quadrature outputs.

By assuming that the limiter leaves the signal-to-noise ratio (SNR) unchanged, although in reality the SNR is altered, and ignoring any ISI effects, the approximate effective E_b/N_o as derived in Appendix A is

$$(E_b/N_o)_{eff} = \frac{(E_b/N_o)_{up} \; (E_b/N_o)_{down}}{(E_b/N_o)_{up} + (E_b/N_o)_{down} + \frac{B}{R}} \tag{2.2}$$

where $(E_b/N_o)_{up}$ and $(E_b/N_o)_{down}$ are the uplink and downlink SNR's multiplied by B/R, respectively [1,17]. If the SNR at the input is large, the limiter doubles the SNR [18, p. 311, Prob. 13]. However, this gain in signal to noise actually cannot be exploited; the effective end-to-end ratio might as well be calculated assuming that this gain is nonexistent. It is demonstrated in Appendix A that this $(E_b/N_o)_{eff}$ is within a decibel of the true E_b/N_o, ignoring any ISI effects of the filter. The terminology "balanced" uplink and downlink simply means that $(E_b/N_o)_{up} = (E_b/N_o)_{down}$.

In a system using FLEETSAT the links will usually be unbalanced because of different terminal capabilities [1]. Note from (2.2) that if one of the links is much noisier than the other, then $(E_b/N_o)_{eff}$ is approximately equal to the E_b/N_o of the noisy link. If the links are balanced, then $(E_b/N_o)_{eff}$ is comparable to and at most 3 dB smaller than the link E_b/N_o's. In this report, B/R will usually be small compared to the sum of the link E_b/N_o's.

Estimates of the bit error probability P_b obtained by counting errors will be plotted as a function of $(E_b/N_o)_{eff}$ in Section III. For the sake of comparison solid curves representing the theoretical bit error probability

$$P_b = \frac{1}{2} \text{ erfc } (\sqrt{(E_b/N_o)_{eff}}) = \frac{1}{\sqrt{2\pi}} \int_{\sqrt{2(E_b/N_o)_{eff}}}^{\infty} e^{-x^2/2} dx \qquad (2.3)$$

for coherent demodulation of equally-likely antipodal signals in AWGN will also be shown. The degradation from this theoretical curve due to the narrow bandpass-limiting channel will be the principal quantity of interest.

The nonlinearity introduced by the bandpass limiter severely hampers analysis in general. Although much can be done to mitigate ISI in a linear system [15, 19], and though bandpass limiters (without filter distortion) have been analyzed to a considerable degree [17, 20, 21], the narrow bandpass-limited channel is better handled through simulation or experimentation. The approaches taken in much of the literature dealing with linear channels even resort to simulation [3], experimentation [9], or restricted analyses and numerical methods [7, 8, 10, 11]. Since the satellite components were unavailable, we chose simulation.

On the other hand, a promising theoretical approach has just appeared [22] for handling a bandlimited nonlinear channel for the special case of BPSK and downlink noise only using the Forney scheme [15]. Since [22] is in the realm of more complex receiver structures mentioned earlier, an analysis of this sort will be deferred. Unfortunately, it will probably be difficult to extend [22] to more attractive modulations such as QPSK, let alone MSK or SQPSK.

We know of just three other investigations [4-6] that are closely related to our objective of communicating at high data rates with the model of Fig. 1.1. However, none of these efforts, which were experimental in nature, permitted both uplink and downlink noise sources simultaneously or included all the modulations we consider.

2.1.3 Digital Processing

Several different digital filters were employed in the simulation. Frequency sampling techniques were used to design some of the filters. The bilinear transformation from the analog to digital domain was used in other design procedures for the Chebyshev, Butterworth and elliptic filters [23,24]. This transformation avoids the problem of aliasing of the analog frequency spectrum in the digital representation of a system of discrete uniformly-spaced samples. But the effect of the aliasing on the accuracy of the model is small if the analysis bandwidth W is sufficiently large.

A baseband simulation involving complex signals and noise is more convenient mathematically and is more efficient than a bandpass one because a much smaller sampling rate is required. The channel filter 3-dB bandwidth B should be distinguished from the analysis bandwidth W, the complex sampling rate of our baseband digital simulation model. In order to insure a reasonably accurate approximation to the bandpass situation, W must be significantly larger than the greater of B and the 3-dB bandwidth of the signaling spectrum B_s, since the ideal bandpass limiter generates extensive intermodulation products. We have decided on the rule-of-thumb

$$W \gtrsim 4 \max \{B, B_s\} \qquad\qquad (2.4)$$

as an adequate analysis bandwidth.

Some experimentation was performed to test the sufficiency of this rule-of-thumb. We found that doubling complex sampling rates approximately equal to the right-hand side of (2.4) did not change the measured error probabilities appreciably. Other investigations of binary matched-filter detection have concluded that four complex samples per data bit are adequate [25, 26]. Although this conclusion is not necessarily valid with the limiter present or when B_s is significantly larger than B, it is consistent with (2.4), since the 3-dB bandwidth of BPSK is approximately 0.9R (see Section 2.2.2).

2.2 Modulation Schemes

Only modems that achieve the theoretical matched-filter performance for antipodal signals and the distortionless channel in AWGN have been considered. The modulations to be simulated are denoted by the following acronyms [27]:

BPSK   Binary Phase Shift Keying

QPSK   QuadriPhase Shift Keying

SQPSK   Staggered or offset QPSK; same as QPSK except that phase changes are restricted to 0 or $\pm\pi/2$ and may occur twice as often

AQPSK   Alternating QPSK; same as SQPSK except that phase changes are restricted to $\pm\pi/2$

MSK   Minimum Shift Keying; continuous-phase binary frequency shift keying with a frequency separation of R/2; same as SQPSK except that the quadrature modulating waveforms are sinusoidal rather than rectangular in shape

CPQFSK   Continuous-Phase QuadriFrequency Shift Keying with a frequency separation of R/4.

Typical modulation waveforms for every scheme but BPSK are drawn in Fig. 2.2. BPSK is like one channel of QPSK but with half the intersymbol spacing for the same data rate.

2.2.1 Special Properties

Alternating QPSK is of special interest for symbol timing acquisition and tracking because a phase transition is guaranteed for every data bit. AQPSK also has a built-in immunity to first-order ISI effects [28].

Staggered QPSK, MSK and AQPSK are distinguished by the kindly way an ideal bandpass limiter treats their filtered waveforms. Rhodes' computer simulations [29] showed that SQPSK and MSK retain their bandlimited spectra with low sidelobes after ideal bandpass limiting, in contrast to QPSK. Other experimentation has shown that the limiter builds up the sidelobes of filtered AQPSK but to magnitudes well below their prefiltered levels [28].

When there is little or no sidelobe build-up, the output of the satellite power amplifier, which the bandpass limiter represents, need not be filtered as much, if at all. Even without such filtering, however, the sidelobe build-up with QPSK is not very significant in terms of measured error probabilities as will be seen in Section III.
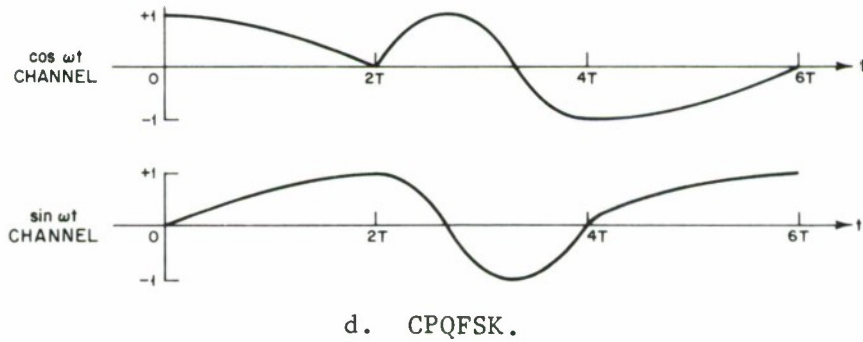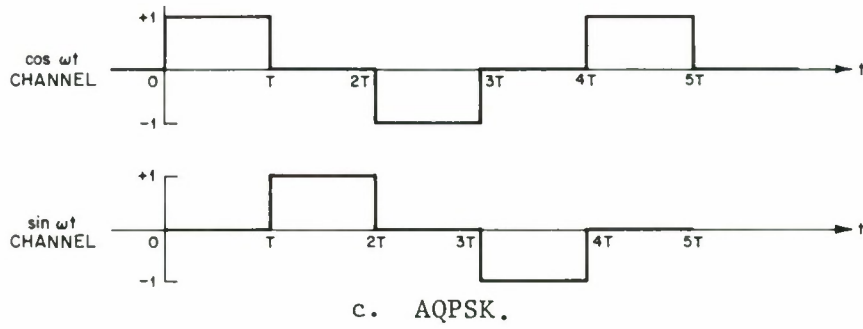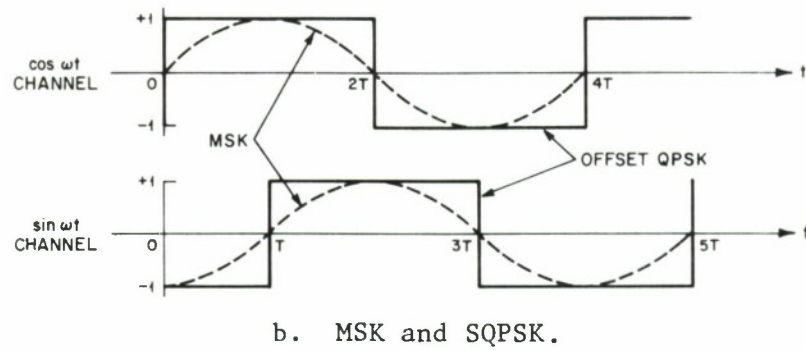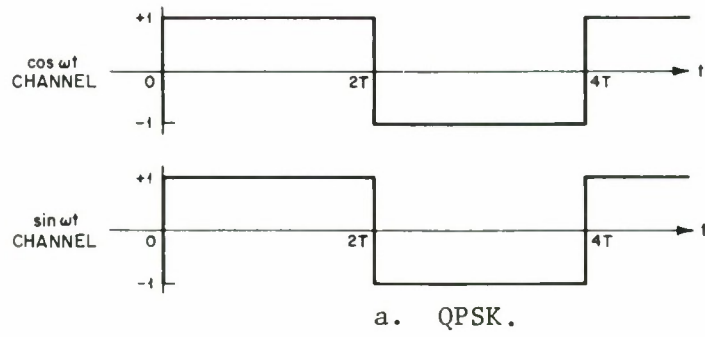
21

a. QPSK.

b. MSK and SQPSK.

c. AQPSK.

d. CPQFSK.

Fig. 2.2. Modulation waveforms.

2.2.2 Signal Bandwidths

We should be cognizant of the relative signaling bandwidths of different modulations when interpreting the data of Section III. Let the double-sided r-dB bandwidth of a baseband signal be defined as twice the frequency where the power spectral density first falls to r dB below the f=0 value. And let the double-sided zero-crossing bandwidth be twice the frequency of the first spectral null. Then for an infinite sequence of uniformly-distributed symbols, several of these bandwidths are listed in Table 2.1 for each modulation scheme.

We are assuming without verification[*] that AQPSK has the same spectrum as BPSK [28], and that SQPSK has the same spectrum as QPSK [5,29]. Both BPSK and QPSK have the classical $(\sin r/r)^2$ spectrum with a zero-crossing bandwidth of exactly twice the symbol rate [30].

The zero-crossing bandwidth for MSK is exactly 3R/2, and the MSK 3-dB bandwidth of Table 2.1 is accurate [31] . The other bandwidths for MSK and all the CPQFSK bandwidths are only approximations. The CPQFSK bandwidths were taken from curves in [32] . General expressions for continuous-phase FSK spectra are given in [32, 33].

From Table 2.1 we see that the QPSK bandwidth is half that of BPSK, as is well known, and that the r-dB bandwidth of MSK is less than 1.5 times that of QPSK. However, MSK generally has a much smaller fraction of out-of-band energy than QPSK [5]. The spectrum of CPQFSK is also quite compact because of the minimum signaling frequency separation for orthogonality and the phase continuity [31, 32] .

---

[*]This statement may be an assumption of fact.

TABLE 2.1

DOUBLE-SIDED SIGNALING BANDWIDTHS FOR INFINITE UNIFORMLY-
DISTRIBUTED DATA SEQUENCES

Modulation	Bandwidth (R is the data rate in bits per sec)			
	3-dB	13-dB	20-dB	Zero-Crossing
BPSK, AQPSK	0.886R	1.70 R	1.92R	2R
QPSK, SQPSK	0.443R	0.852R	0.96R	R
MSK	0.595R	1.13 R	1.32R	$3R/2$
CPQFSK	0.63 R	1.59 R	1.62R	$\approx 2.5R$

24

III. PERFORMANCE ANALYSIS

The simulation results using an IBM 370/168 computer are presented in this section. Unless stated otherwise the data and Gaussian noise sequences were selected using the nearly uniformly distributed pseudorandom number generator [34]

$$K_{n+1} \equiv 11^5 K_n \pmod{2^{31} - 1} \qquad (3.1)$$

where K_1 is a 9-digit integer, and a polar method for normal deviates [35]. The same sequences were employed when comparing different modulations.[*]

Unless stated otherwise, each datum shown graphically in this section represents about 2000 bit decisions; some runs in Fig. 3.4 were made with 8000 trials for better confidence intervals. Most of the performance estimates are made in the bit error probability range $10^{-3} \gtrsim P_b \gtrsim 10^{-2}$. Then according to (2.3), $(E_b/N_o)_{eff}$'s in the 4 to 10 dB range are of primary interest, allowing for a few dB degradation from the theoretical performance curve.

Typical measurement errors for a 95% confidence level are listed in Table 3.1 for 2000 and 8000 bit decisions per datum. For a given measurement $(E_b/N_o)_{eff}$, let $\hat{L}_-$ and $\hat{L}_+$ be the degradation from the theoretical curve at $(1 - p)\hat{P}_b$ and $(1 + p)\hat{P}_b$, respectively, where $\hat{P}_b$ is the measured error rate and where p specifies the confidence interval. Then the actual loss L is in the range $\hat{L}_- < L < \hat{L}_+$ with probability 0.95.

Some digital filters used in the simulations are listed in Table 3.2.

---

[*] Every modulation scheme was tested in the presence of AWGN only, as a check on the simulation program; performance was always close to the theoretical bit error probability of (2.3).

TABLE 3.1

RANGE OF ACTUAL BIT ERROR PROBABILITY FOR 95% CONFIDENCE LEVEL

$\hat{P}_b$	NUMBER OF BIT DECISIONS				
	2000			8000	
	p	range		p	range
0.010	40%	$0.006 \underset{\sim}{<} P_b \underset{\sim}{>} 0.014$		20%	$0.008 \underset{\sim}{<} P_b \underset{\sim}{>} 0.012$
0.005	55%	$0.0022 \underset{\sim}{<} P_b \underset{\sim}{>} 0.0078$		29%	$0.0035 \underset{\sim}{<} P_b \underset{\sim}{>} 0.0065$
0.001	130%	$0 \underset{\sim}{<} P_b \underset{\sim}{>} 0.0023$		70%	$0.0003 \underset{\sim}{<} P_b \underset{\sim}{>} 0.0017$

26

TABLE 3.2

DIGITAL FILTERS SIMULATED

Index	Type	Phase
1	Chebyshev	Nonlinear
2	Butterworth	Nonlinear
3	FIR[†]	Linear
4	elliptic	Nonlinear
5	FIR	Nonlinear
6	FIR	Cubic

† Finite Impulse Response

27

The Chebyshev, Butterworth and elliptic filters were implemented in the time domain. The Finite Impulse Response (FIR) filters were realized by a fast convolution method via the frequency domain. Additional information is given in Appendix B.

For programming convenience an integral number of complex samples per symbol was guaranteed in the simulations. An adequate analysis bandwidth was used for all the results reported in this section. (See Section 2.1.3.)

The principal parameter of interest for a set of data will be the 3-dB filter bandwidth to data rate ratio B/R. Different modulations will always be compared using the same filter. We will emphasize results for the filters that come closest to the FLEETSAT filter. There is an overall performance comparison among different filters in Section I.

3.1 Linear-Phase FIR Filter

Filter 3 of Table 3.2 was the first to be designed [36] and simulated. This linear phase filter is used as a baseline for comparison, especially with respect to results for nonlinear phase filters. Its frequency response and the associated performance data for B/R = 0.69 and 0.46 are given in Figs. 10-12 of [37]. There it was concluded that:

    A.   A data rate of 32 kbps is feasible with little or no performance degradation for QPSK, SQPSK, AQPSK, or MSK;

    B.   A data rate of 48 kbps is feasible with only a slight increase ($\widetilde{<}$1 dB) in degradation for SQPSK and MSK; the

28

degradation increase for QPSK and AQPSK is approximately 1 dB and 2 dB, respectively, at this rate;

C. Neither BPSK nor CPQFSK is feasible with acceptable performance degradations at data rates of 32 kbps or above, although CPQFSK performed significantly better than BPSK;

D. For bit-error probabilities down to 10^{-3} and data rates of 32 kbps or above, the best performance is achieved by MSK followed by SQPSK, QPSK, AQPSK, CPQFSK, and BPSK in order of increasing degradation.

These degradations are optimistic, mainly due to the linear phase of filter 3, as we shall see when exploring nonlinear-phase filters.

The predominance of errors for CPQFSK resulted from signaling with the two frequencies at the band edge, where more signal distortion is to be expected. The inferior performance of BPSK is attributable to the facts that the signaling bandwidth of BPSK is twice that of QPSK (see Table 2.1) and that phase transitions are always of 180 degrees with BPSK modulation.

Rhodes [29] explains how polarity changes in the bandlimited signal with these 180-degree phase shifts cause destructive ISI and a sharp decrease in the signal envelope. The hard-limiting action of the bandpass limiter tends to restore the signal envelope to its prefiltered value while maintaining the rapid phase change. Thus, we have a spectral sidelobe build-up with BPSK as with QPSK (see Section 2.2.1).

Although AQPSK apparently has the same bandwidth as BPSK, there is less sidelobe build-up, evidently because AQPSK has only 90-degree phase changes.

29

This may help explain why AQPSK performs better than BPSK but the built-in immunity of AQPSK to ISI mentioned in Section 2.2.1 is a more likely explanation. BPSK has none of this immunity.

In comparing the performance of SQPSK and QPSK, which apparently have the same bandwidth, we see from conclusion B above that the sidelobe build-up effect is relatively minor because it can account for less than a 1-dB degradation with filter 3.

Tests between fixed and pseudorandom data sequences were run for MSK, SQPSK, AQPSK and QPSK with B/R = 0.69. For fixed sequence "1" the modulating data streams alternated between +1 and -1 on both quadrature channels; for sequence "2" one data stream alternated while the quadrature stream was held constant. These sequences were likely candidates for generating a maximal amount of ISI and/or crosstalk (see Section 2.1.2). The crosstalk phenomenon due to the bandpass limiter has been verified experimentally [5, 38].

With MSK and filter 3, sequence 1 yielded performance a fraction of a decible worse than a pseudorandom data stream, but sequence 2 did slightly better than a pseudorandom sequence. With SQPSK sequence 2 performed about 1 dB worse than sequence 1 but not any worse than a pseudorandom sequence. With AQPSK sequence 2 was slightly worse than 1 but neither sequence appeared to be as bad as a pseudorandom sequence. Thus, these contrived sequences were not harmful to the offset modulations. However, sequence 1 yielded a 1-dB degradation over pseudorandom performance with QPSK.
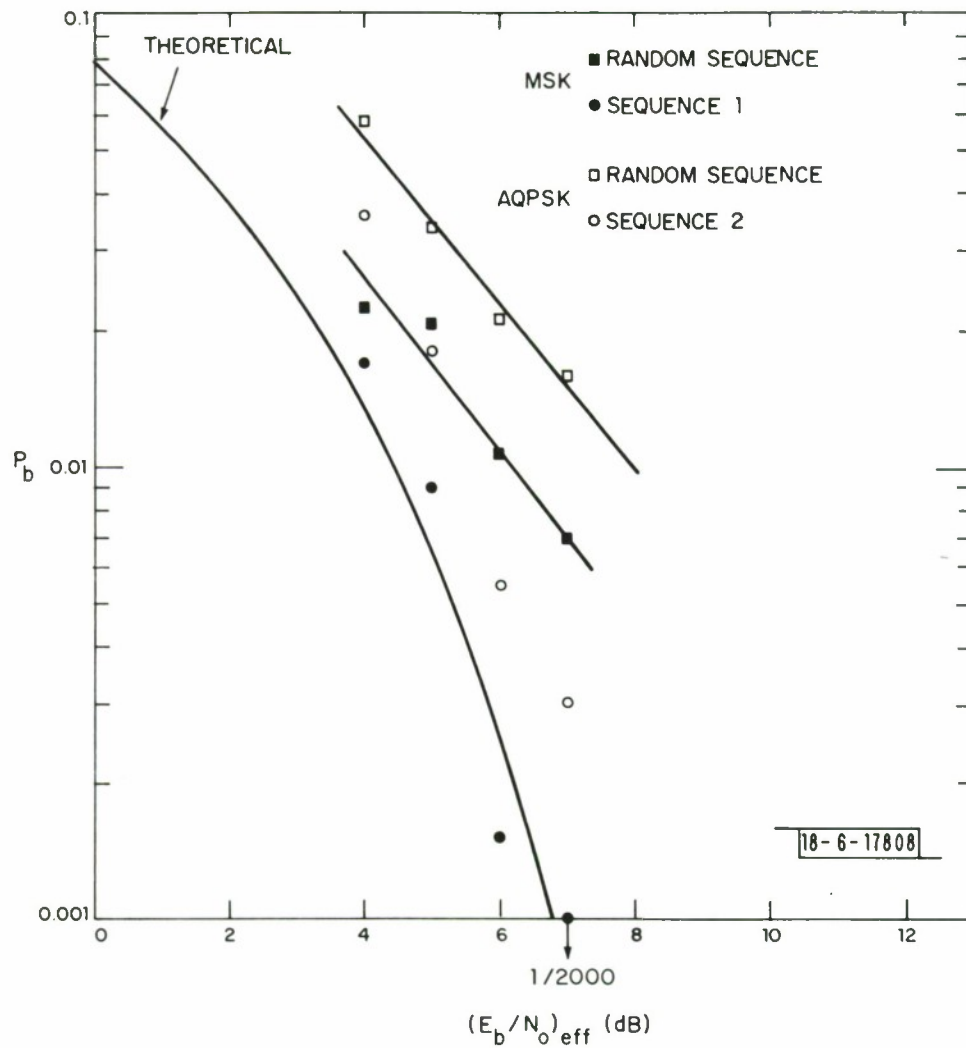
3.2 Butterworth and Chebyshev Filters

With nonlinear-phase Butterworth and Chebyshev filters, we found that

30

sequences 1 and 2 were far from the worst-case inputs for MSK and AQPSK, respectively. As shown in Fig. 3.1, pseudorandom sequences gave many more errors than these fixed sequences. Therefore, it is not obvious what the worst-case data sequence would be for a given offset modulation and satellite model.

Note from Fig. 3.1 that AQPSK performance is approximately 2 dB and 2.5 dB worse than MSK for the Butterworth and Chebyshev filters, respectively. Also observe that the losses for the Chebyshev filter are about 1 dB worse than the Butterworth filter, even though the data rate is 13% smaller. As explained in Section I the Butterworth filter characteristics (see Appendix B) are closer to those of the FLEETSAT filter.

In Fig. 3.1a we see that MSK suffers a 2-dB degradation for $P_b \approx 10^{-2}$ and B/R = 0.54. Comparing this with the filter-3 data (see Fig. 1.3b), the nonlinear phase of the Butterworth filter is probably responsible for no more than 1 dB of this performance loss, with the slightly faster spectral roll-off accounting for the rest.

Additional data gathered under the conditions of Fig. 3.1 except for unbalanced links was not sufficiently different from the balanced case to warrant graphical display. For a noisy uplink and good downlink $((E_b/N_o)_{down}$ = 20 dB) we observed about 1 dB of additional degradation compared to the balanced case. With a good uplink $((E_b/N_o)_{up}$ = 20 dB) and a noisy downlink, performance was about the same as in the balanced case except with MSK and the Butterworth filter, where an additional loss of about 1 dB was observed.

a. Butterworth filter; B/R = 0.54.

Fig. 3.1. MSK and AQPSK performance for Butterworth and Chebyshev filters, bandpass limiter, random and non-random data, and balanced links.
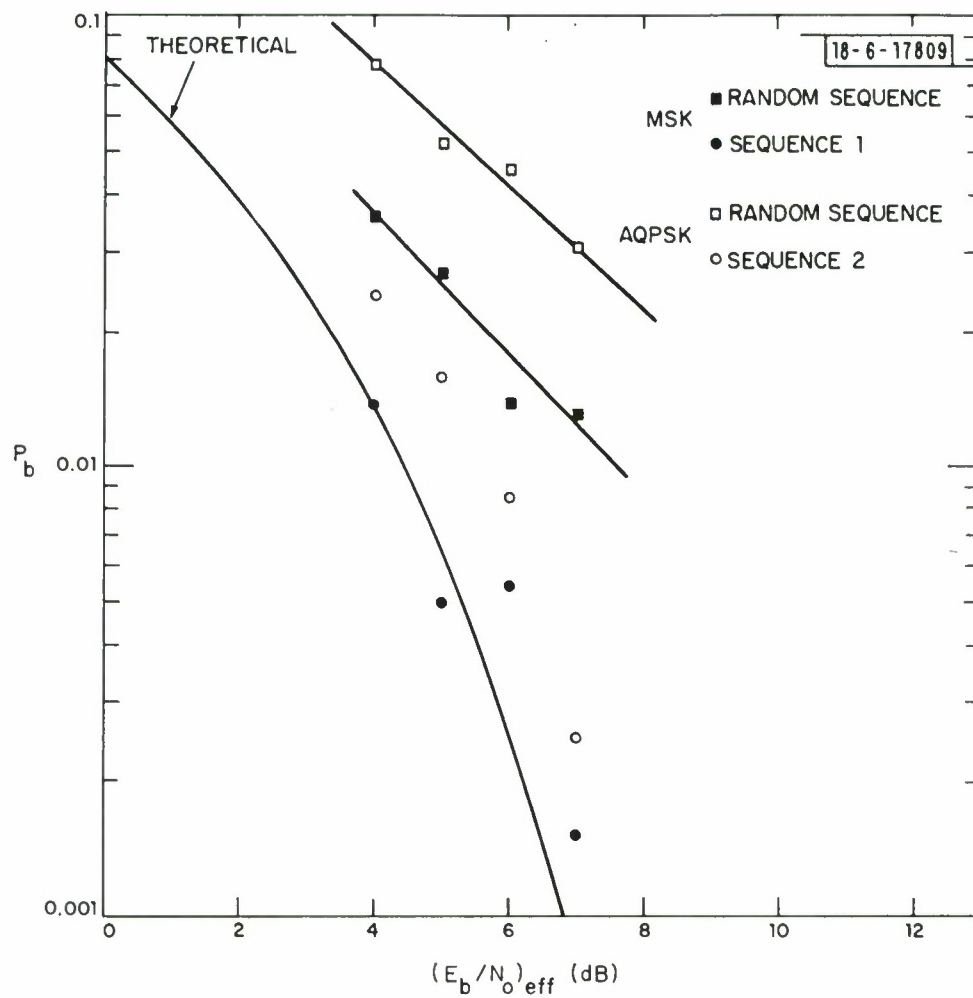
b. Chebyshev filter; B/R = 0.62.
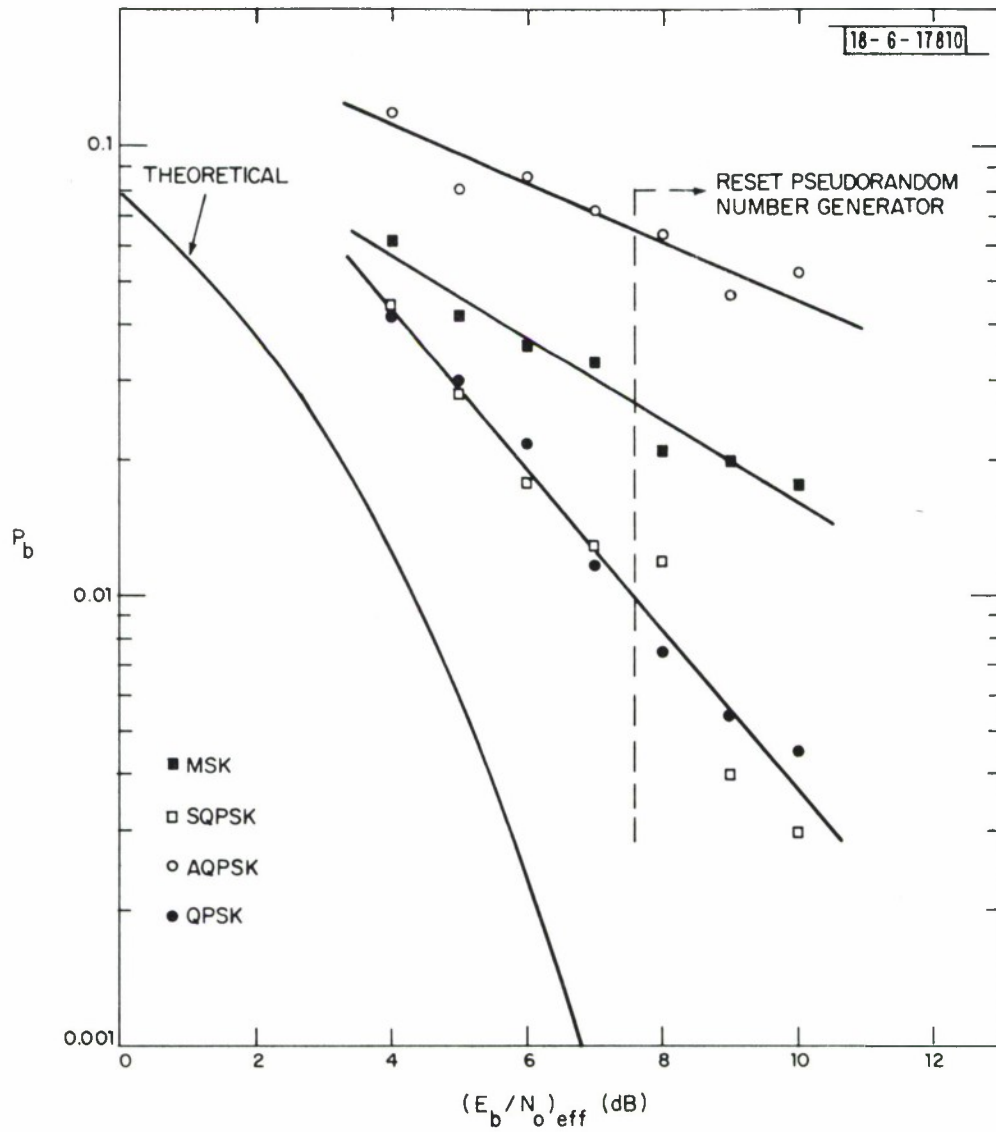
Fig. 3.1. Continued.

3.3 Elliptic Filter

An elliptic filter with about the same spectral roll-off but a much more
nonlinear phase characteristic (see Appendix B) was simulated next. By com-
paring the MSK and AQPSK performance of Fig. 3.2a with that of Fig. 3.1,
we see that this filter represents a pessimistic extreme in the same way that
the linear-phase FIR filter represented an optimistic extreme. As explained
in Section I the Butterworth filter and the 12-degree version of filter 6 to
be discussed later are closer to the FLEETSAT filter. Nevertheless, we include
the data of Fig. 3.2 as an interesting comparison to the Butterworth and
Chebyshev simulations.

At 3/4 the data rate the performance loss for MSK in Fig. 3.2a is reduced
to 2 dB in Fig. 3.2b but the loss for AQPSK is still unacceptable. This is the
only filter simulated for which the MSK performance was significantly worse
than any of the other modulations.

The data of Fig. 3.2a for MSK and AQPSK were basically unchanged by a
four-fold increase in the sampling rate using an elliptic filter with other-
wise identical characteristics.

With fixed data sequence 1 and the conditions of Fig. 3.2a, QPSK yielded
just a few more errors than a pseudorandom sequence. Sequences 1 and 2 both
resulted in less than a 1-dB loss for MSK, as did sequence 1 for SQPSK and
AQPSK; for SQPSK sequence 2 performed worse but still significantly better
than a pseudorandom stream, and with only a 1.5-dB loss for AQPSK. For the
smaller data rate of Fig. 3.2b, sequence 1 for MSK and sequence 2 for SQPSK
and AQPSK performed better than but much closer to a pseudorandom sequence,

a. B/R = 0.72.

Fig. 3.2. Performance for elliptic filter, bandpass limiter, random data, and balanced links.
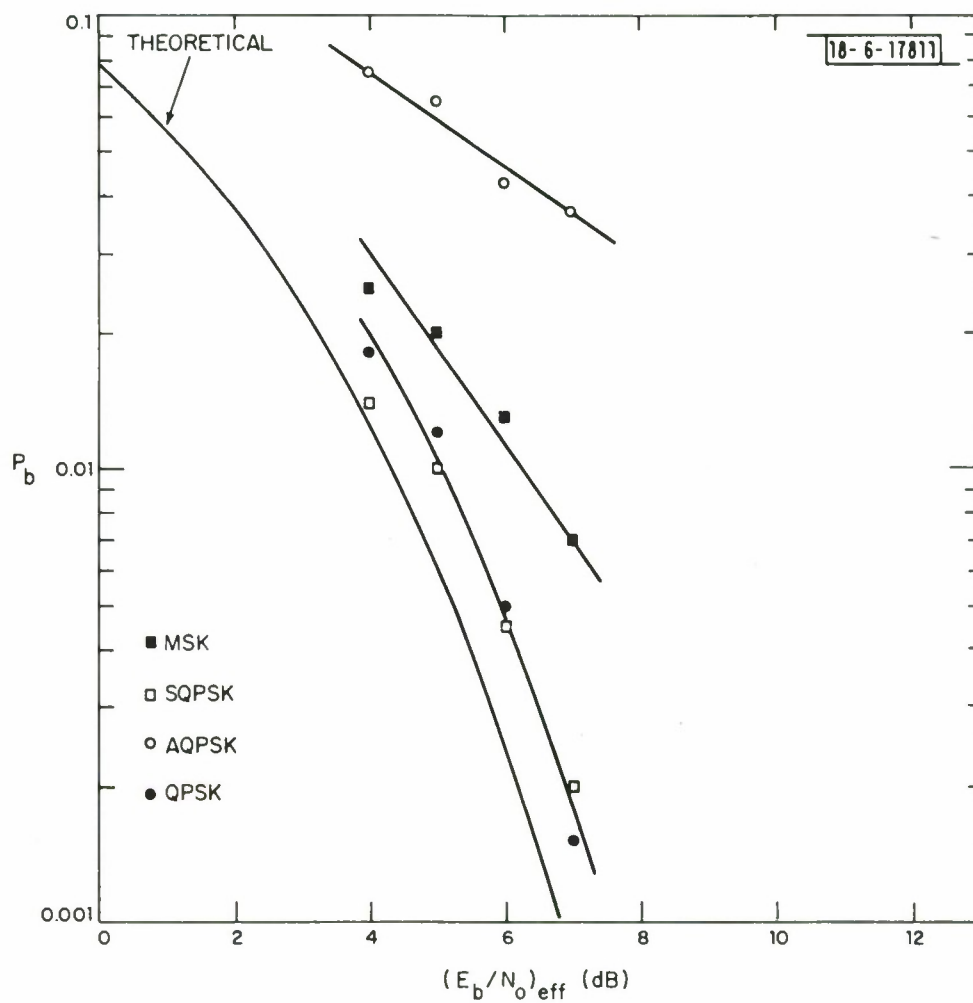
b. B/R = 0.96.

Fig. 3.2. Continued.

as would be expected. Thus, neither fixed sequence is a worst-case data stream for offset modulations and our satellite model. Hence, all simulations in the sequel employed pseudorandom data.
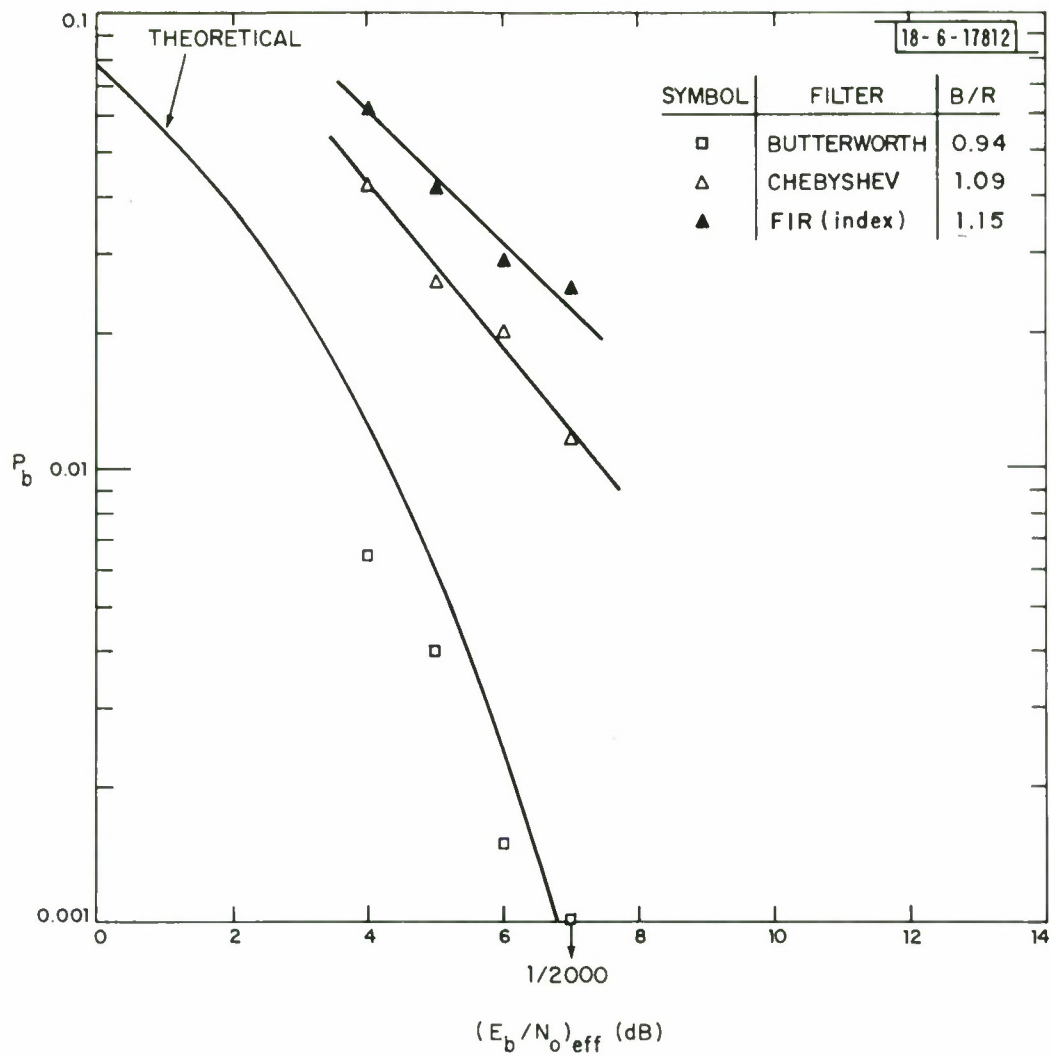
3.4 BPSK Performance

We must drastically reduce the data rate with BPSK to get acceptable performance losses as shown in Fig. 3.3. With the exception of the filter-3 data which shifted to the right about 1 dB, the performance for a solid up-link $((E_b/N_o)_{up} = 20$ dB) is close to that of Fig. 3.3a. In these cases the faster spectral roll-off and nonlinear phase of the Butterworth filter are each responsible for about a 1-dB degradation over filter 3, taking discrepancies in B/R ratios into account. This is consistent with earlier MSK results.

In Fig. 3.3b, where the uplink E_b/N_o varies between 5 and 7 dB, the Chebyshev filter degrades almost 1 dB more than in the balanced case. For the noisy uplink case of Fig. 3.3c, the performance for filter 3 and the Butterworth filter is about 1 dB worse than in Figs. 3.3a and b; the Chebyshev and elliptic filters do only a fraction of a decibel worse than before.

We believe that the noticeably smaller losses with balanced links compared to a noisy uplink case are because the bandpass limiter mitigates the ISI introduced by the filter when the uplink is not dominated by noise.
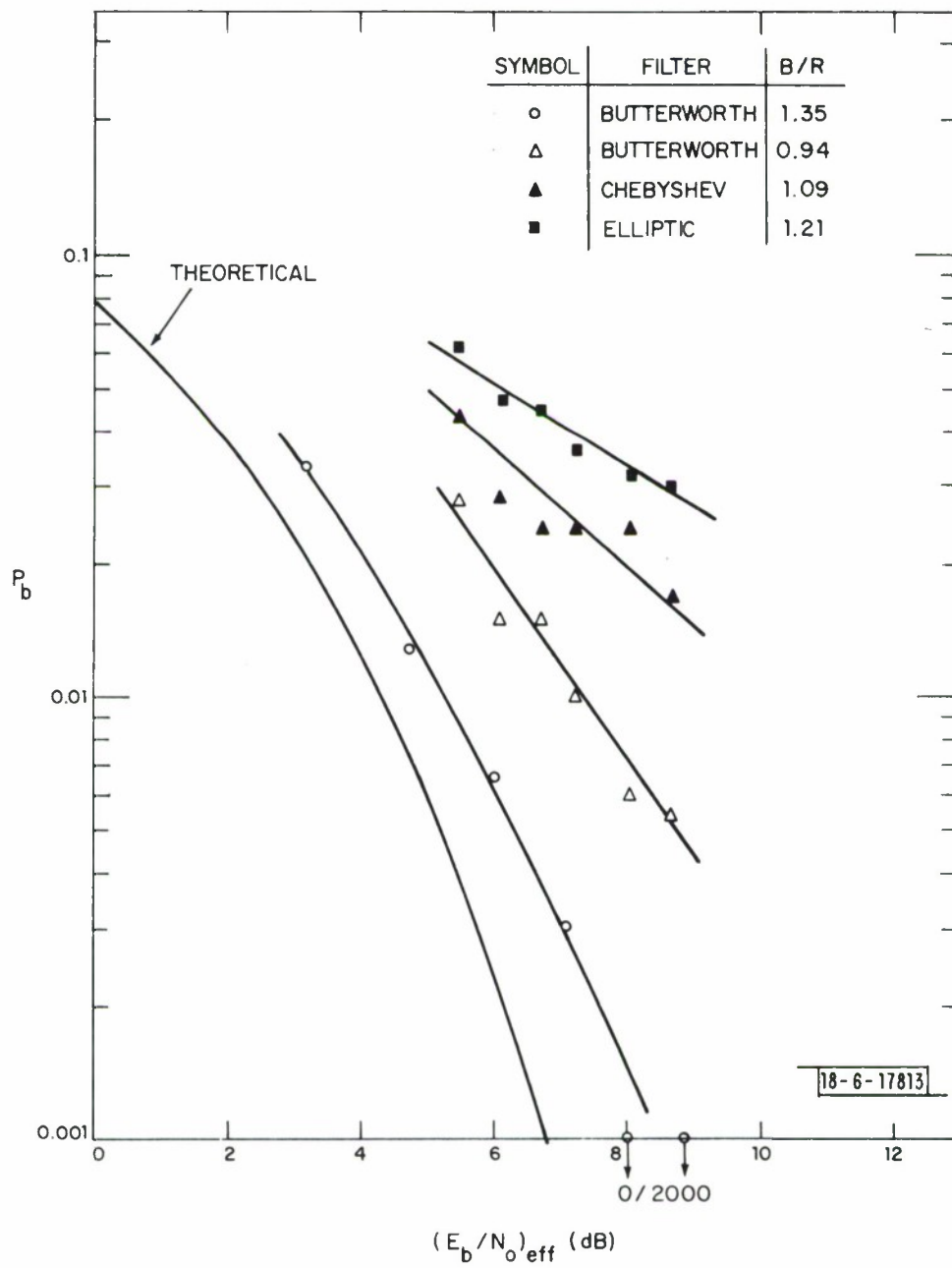
3.5 Nonlinear-Phase FIR Filter

The next model simulated, filter 5 of Table 3.2, has characteristics very close to the FLEETSAT filter (see Fig. 1.2). In an earlier version the phase
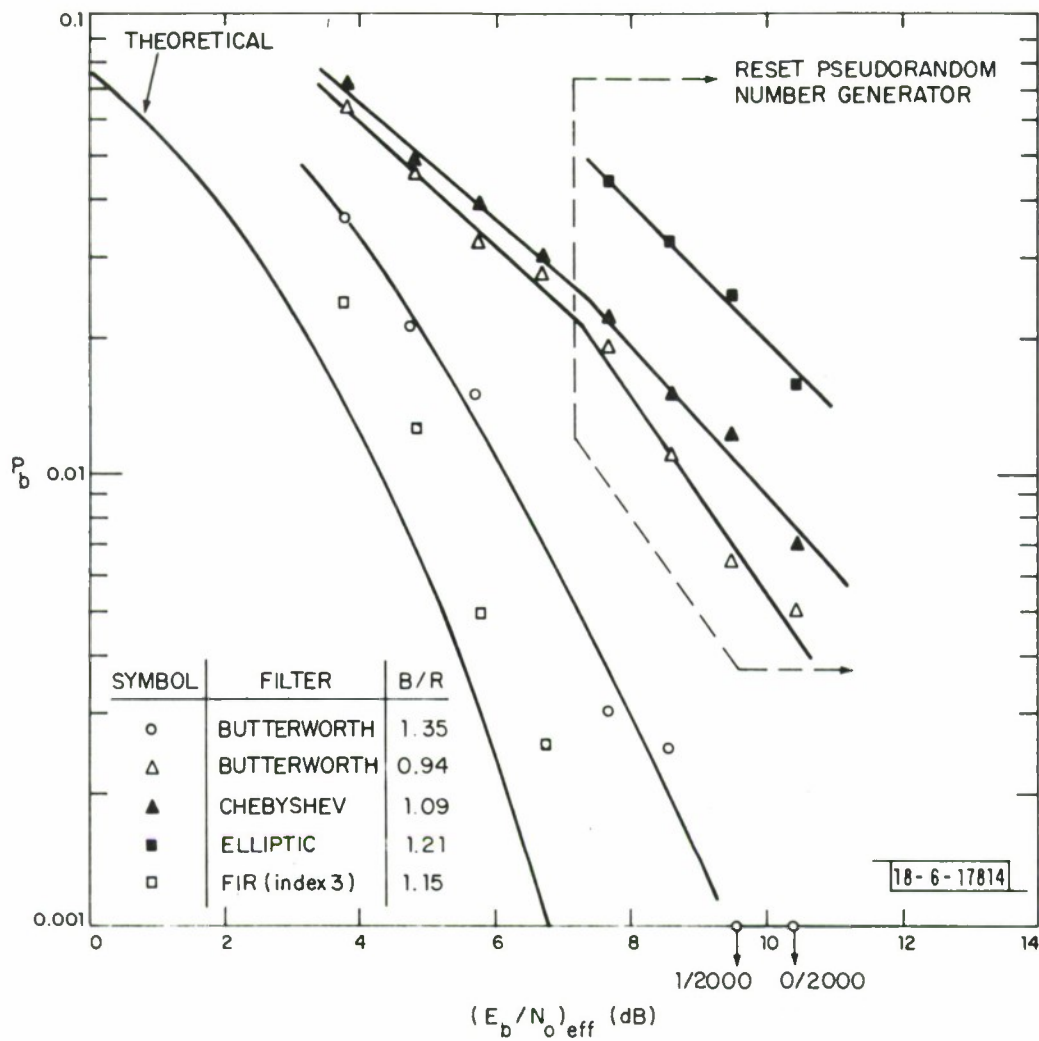
37

a. Balanced links.

Fig. 3.3. BPSK performance for various filters, bandpass limiter, and random data.

38

SYMBOL	FILTER	B/R
o	BUTTERWORTH	1.35
△	BUTTERWORTH	0.94
▲	CHEBYSHEV	1.09
■	ELLIPTIC	1.21

THEORETICAL

P_b

$(E_b/N_o)_{eff}$ (dB)

18-6-17813

0/2000

b. $(E_b/N_o)_{down} = 10$ dB.

Fig. 3.3. Continued.

39

c. $(E_b/N_o)_{down} = 20$ dB.

Fig. 3.3. Continued.

response at the band edges was specified rather arbitrarily in the absence of available phase deviation data and is probably too nonlinear. In this respect the filter-5 simulation data presented in [39] was conservative.

The performance of the latest FLEETSAT filter model (filter 5) is shown in Fig. 3.4 for BPSK, MSK and SQPSK. Most of the points represent 8000 bit decisions. Figures 3.4a and b present data for BPSK and MSK and balanced links where $(E_b/N_o)_{up} = (E_b/N_o)_{down}$; Fig. 3.4c gives data for unbalanced links. The performance of SQPSK was slightly (but not significantly) worse than that of MSK in Fig. 1c and with balanced links, based on data not shown.

For a zero center frequency offset there is less than a one decibel degradation in BPSK for B/R = 1.35. However, the loss increases rapidly with the data rate to about 4 dB at P_b = 0.005 for B/R = 0.94. With MSK there is very little loss for B/R = 0.81 but a 2 or 3-dB degradation for B/R = 0.54.
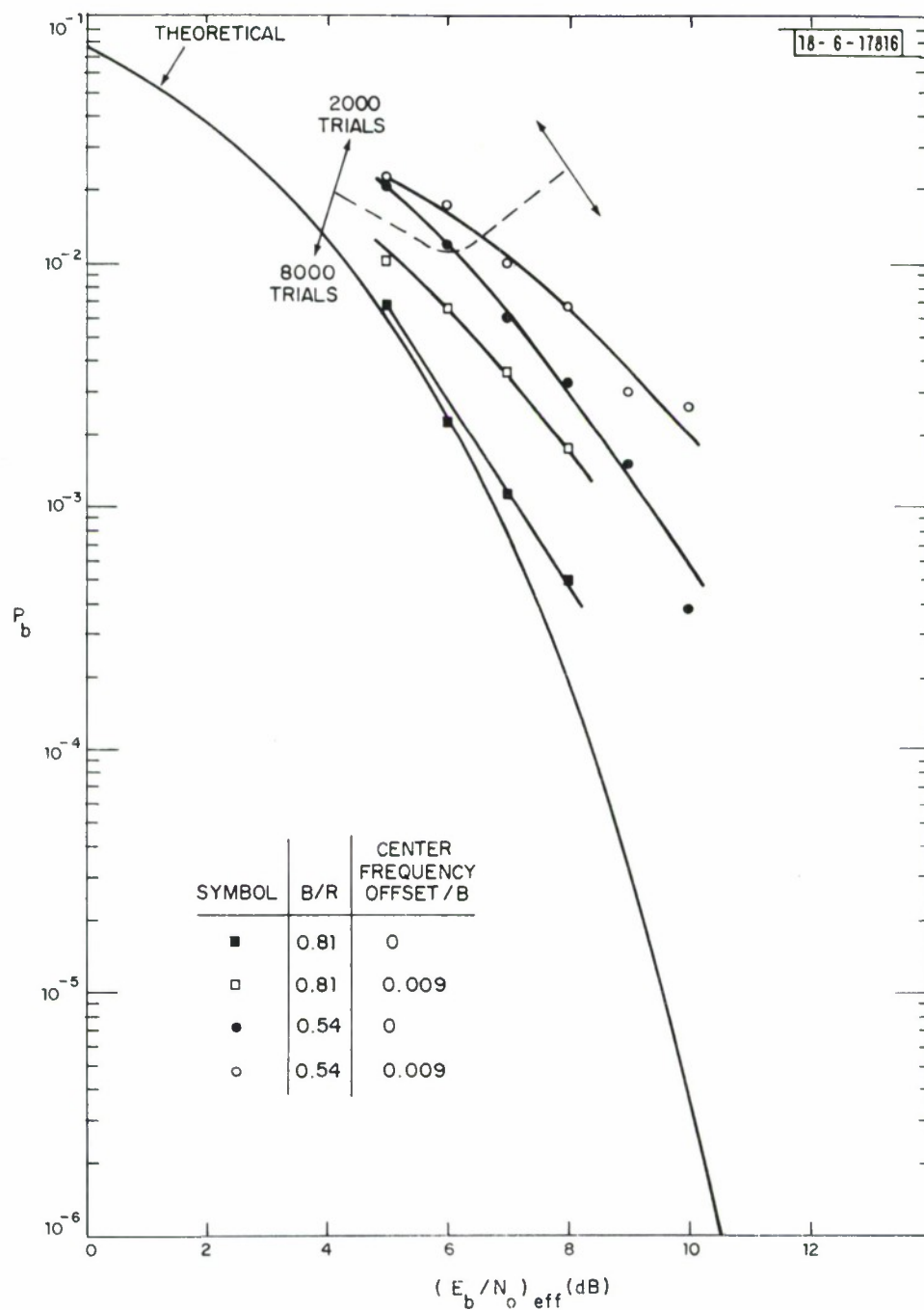
Additional performance losses due to an uncompensated center frequency offset in the FLEETSAT filter are also indicated in Figs. 3.4a and b. A 2% frequency offset relative to the 3-dB filter bandwidth B at B/R = 1.35 seems tolerable for BPSK. But higher percentage offsets mean much larger losses as shown in Fig. 3.4a. Even a 1% frequency offset at B/R = 0.81 and 0.54 means a significant additional loss for MSK and SQPSK, however. Keeping in mind the signaling bandwidth differences for these modulations (see Table 2.1), we conclude that MSK and SQPSK are more sensitive than BPSK to uncompensated center frequency offsets in the FLEETSAT channel.

Figure 3.4c demonstrates that the SNR enhancement of the limiter for a solid uplink cannot be exploited, since the performance loss is no less than with balanced links or a solid downlink. (See Section 2.1.2 and Appendix A.)

41

CENTER
FREQUENCY
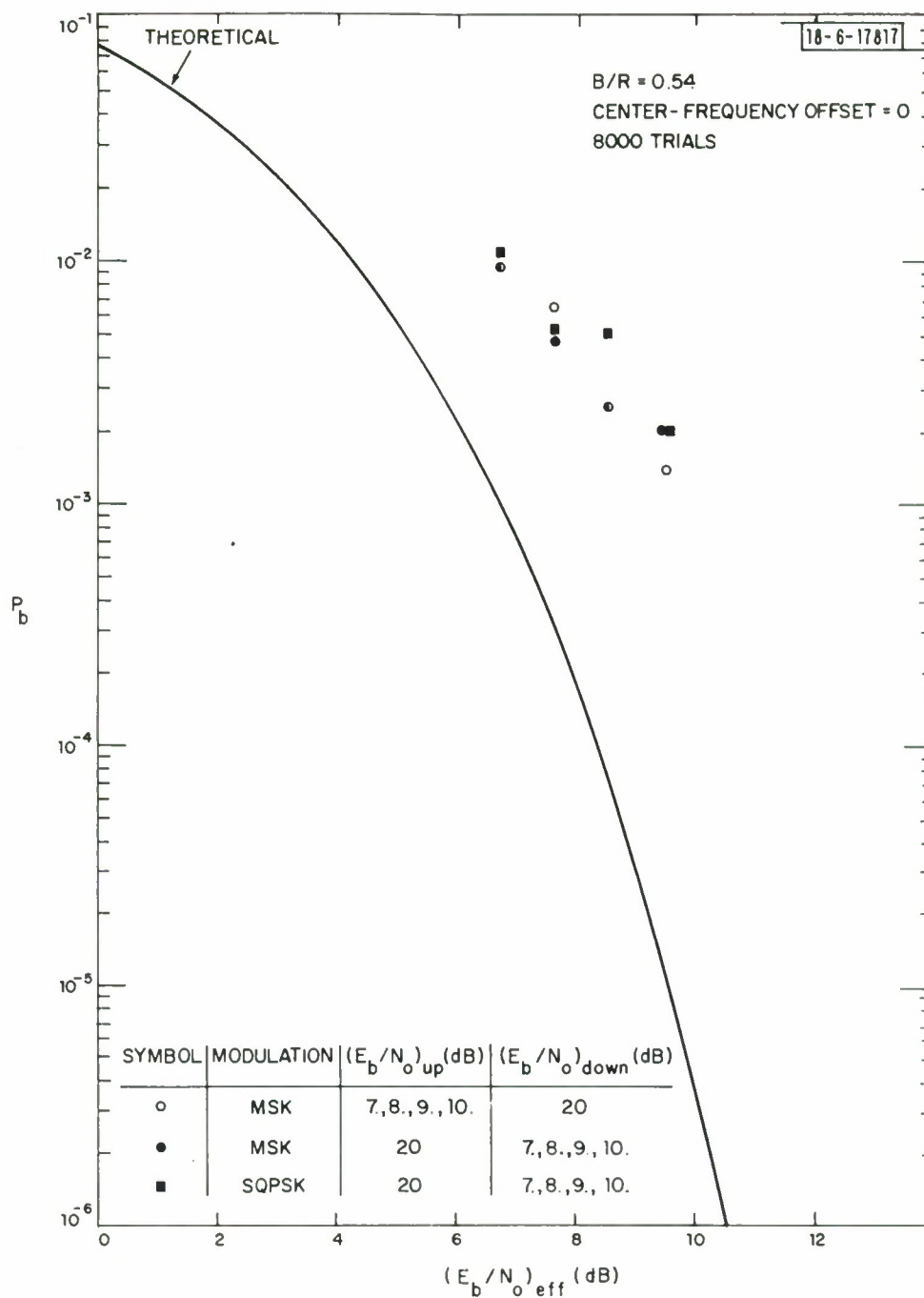| SYMBOL	B/R	OFFSET/B
●	1.35	0
○	1.35	0.018
▲	1.35	0.02B
△	1.35	0.035
■	0.94	0
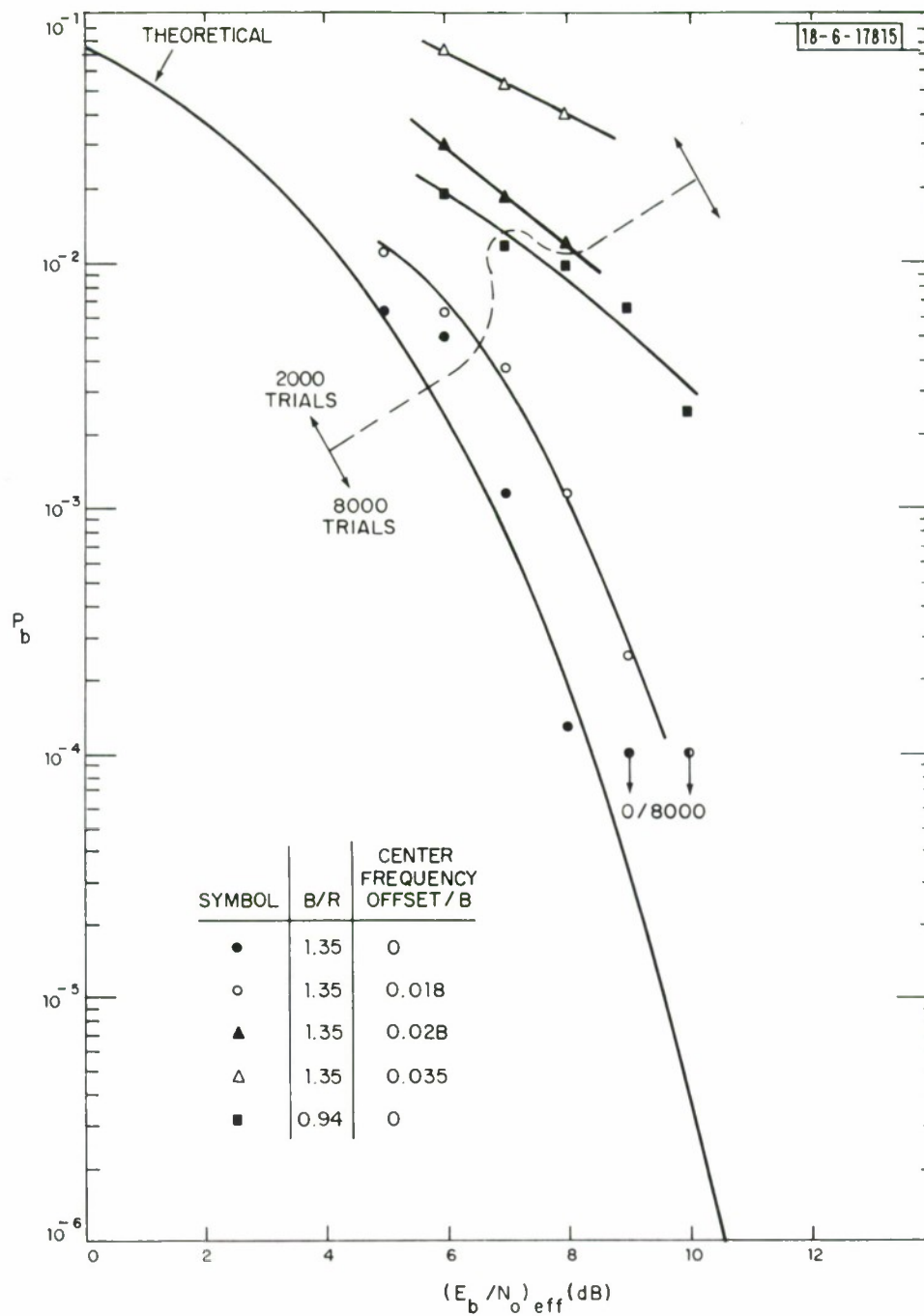
a. BPSK; balanced links.

Fig. 3.4. Performance for FIR filter 5 (closest filter to FLEETSAT), bandpass
limiter, random data and balanced links.

b. MSK; balanced links.

Fig. 3.4. Continued.

THEORETICAL

10^{-1}

18-6-17817

B/R = 0.54
CENTER-FREQUENCY OFFSET = 0
8000 TRIALS

10^{-2}

P_b

10^{-3}

10^{-4}

10^{-5}

SYMBOL	MODULATION	$(E_b/N_o)_{up}$ (dB)	$(E_b/N_o)_{down}$ (dB)
○	MSK	7.,8.,9.,10.	20
●	MSK	20	7.,8.,9.,10.
■	SQPSK	20	7.,8.,9.,10.

10^{-6}

0   2   4   6   8   10   12

$(E_b/N_o)_{eff}$ (dB)

c.   MSK and SQPSK; unbalanced links.

Fig. 3.4.   Continued.

44

3.6 Cubic-Phase FIR Filter

The last filter simulated, FIR filter 6 of Table 3.2 and Appendix B, has an overall magnitude response that is quite faithful to that expected for the FLEETSAT filter and an adjustable linear, quadratic or cubic-phase characteristic. In the nonlinear-phase cases, an arbitrary phase deviation from linearity can be chosen.

Filter 6's performance for B/R = 0.5 and all modulations but BPSK is shown in Fig. 3.5. In Figs. 3.5a and b we compare results for 12 and 36-degree phase deviations at 0.35B to the right of band center. Figures 3.5b and c compare performance for cubic and quadratic phases. Finally, Figs. 3.5b and d show results for different correlation delays.

MSK yields the best performance while CPQFSK does very badly. In contrast to the filter-3 data, there was no predominance of errors when signaling at the two extreme frequencies.

Performance is rather insensitive to a change in correlation delay of 25% of the integration time of 2/R for MSK, SQPSK, QPSK and CPQFSK [27]; previously, a 12.5% change for MSK made little difference with the Chebyshev filter [38]. It is remarkable that a change in the AQPSK correlation delay of 50% of the integration time of 1/R was not more noticeable, but the greater tolerance for first-order ISI would be a contributing factor.

For reasons discussed in Section I we predict a 2 or 3-dB performance loss for B/R = 0.52 MSK or SQPSK and the FLEETSAT model based largely on the 12-degree filter-6, Butterworth and filter-5 simulations.

Worst-case filter-6 performance for BPSK at various B/R ratios is shown
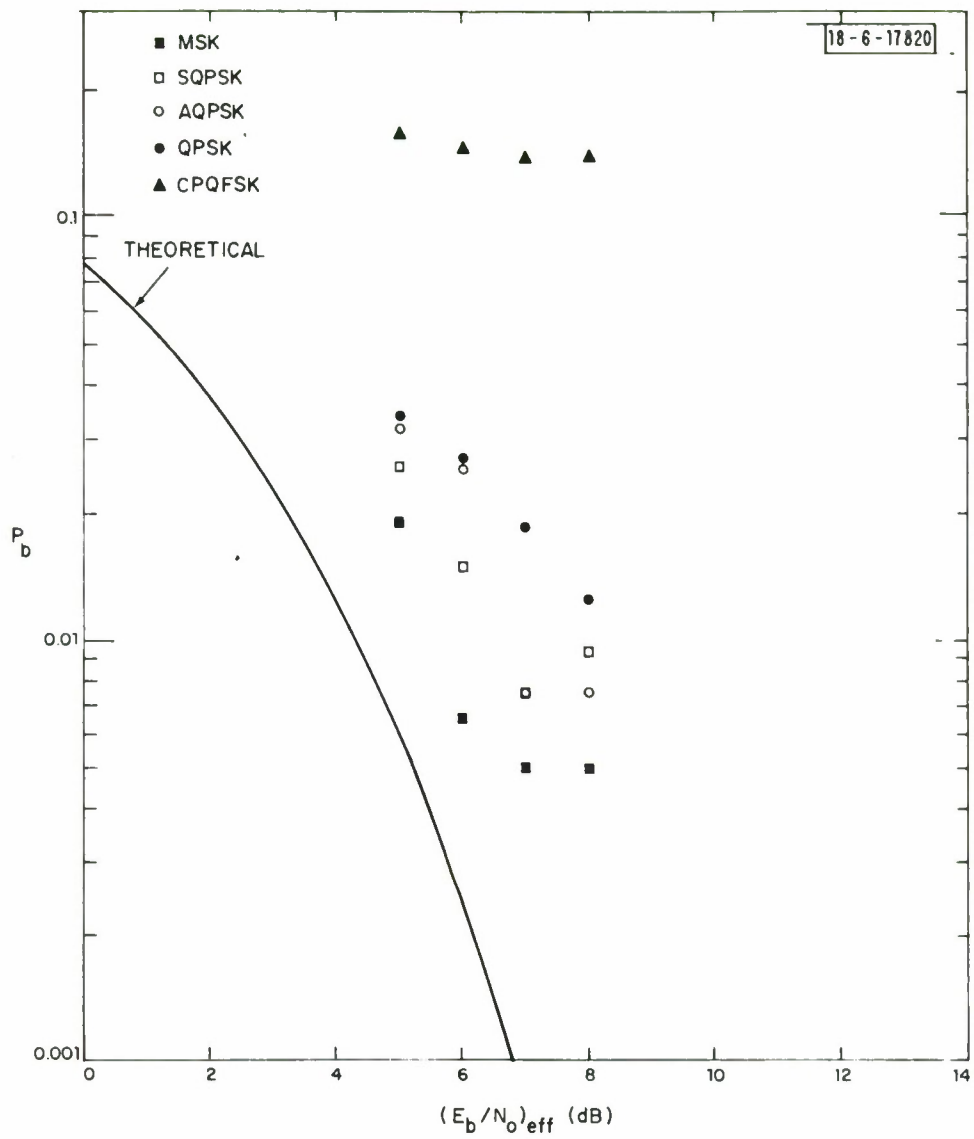
45
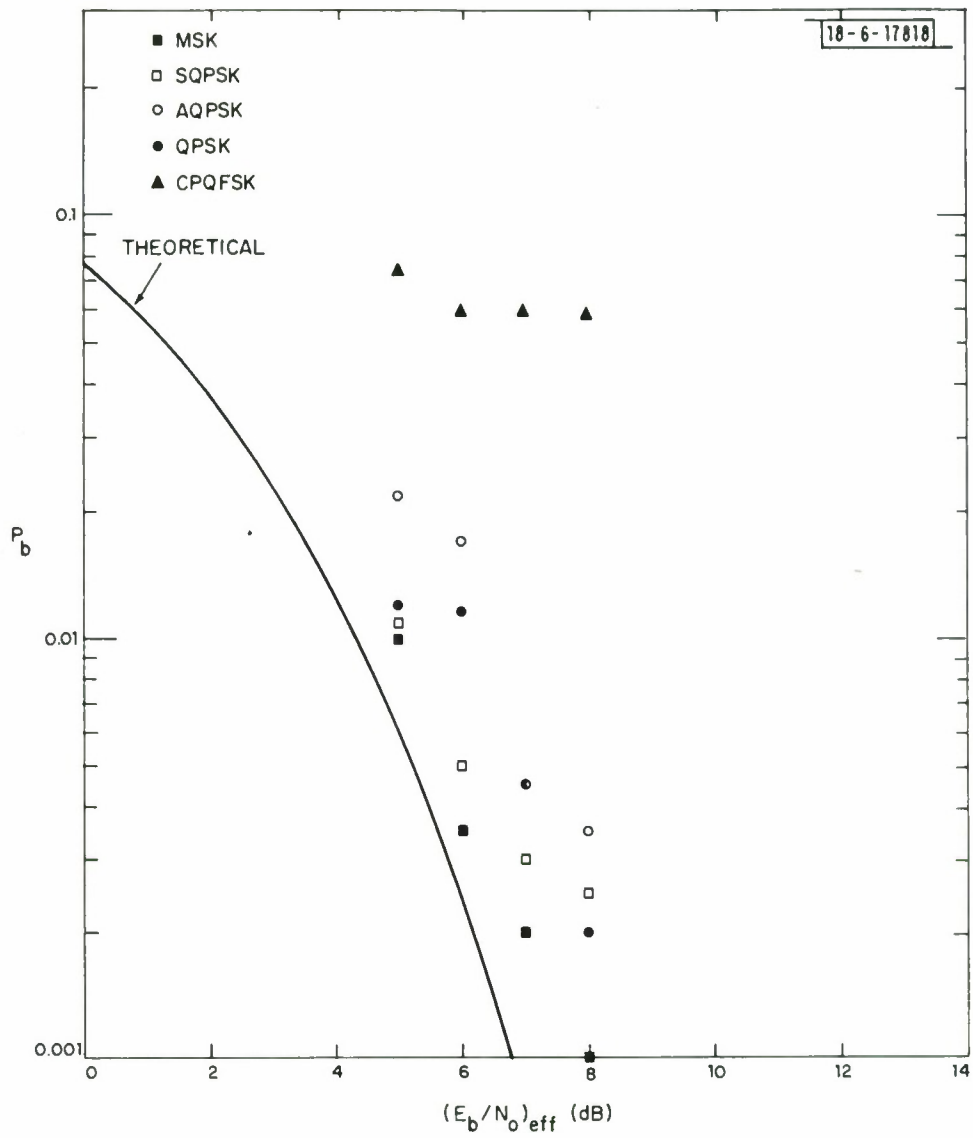
a. Cubic phase, 12° deviation, 15.7/R delay.

Fig. 3.5. Performance for FIR filter 6, various modulations, bandpass limiter, random data and balanced links (B/R = 0.505, deviation at 0.35B).
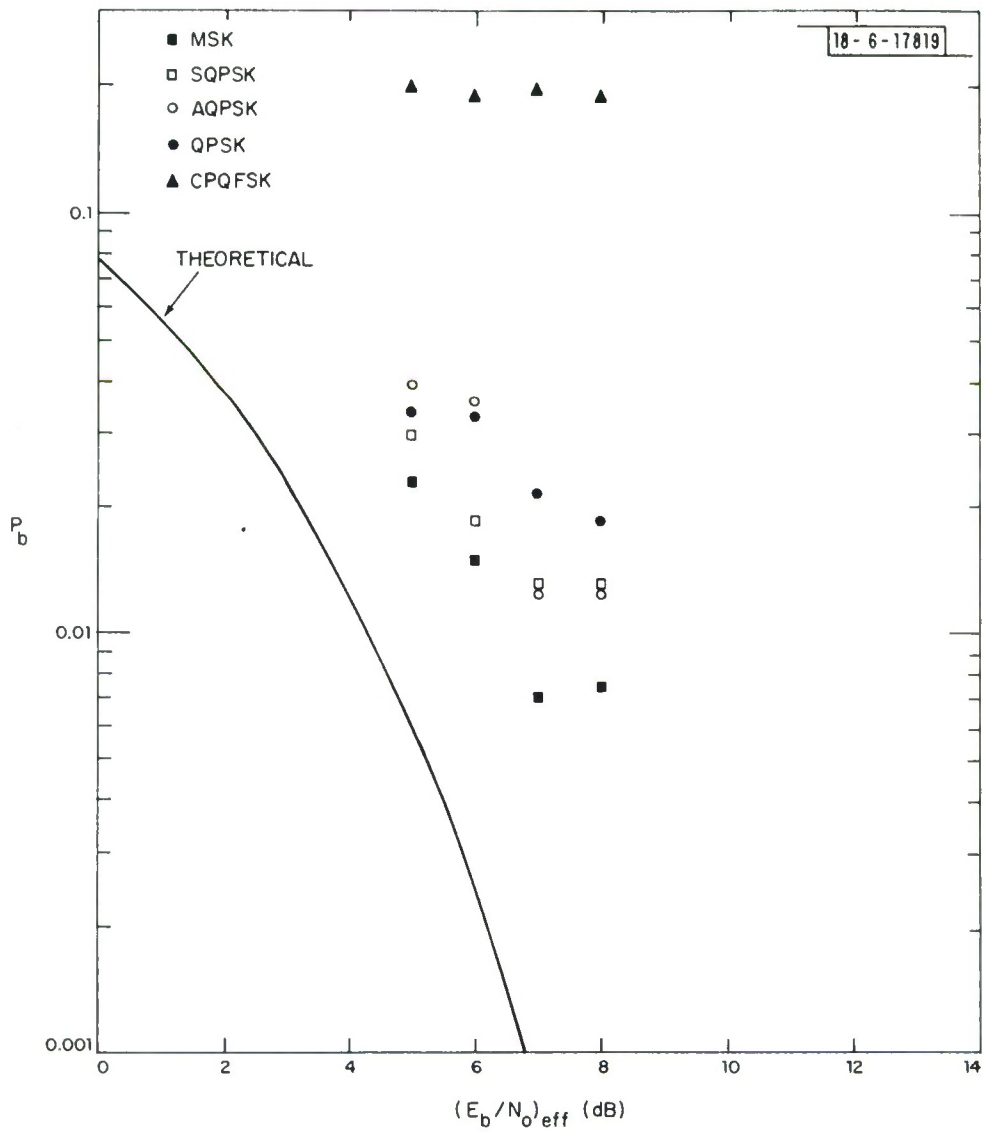
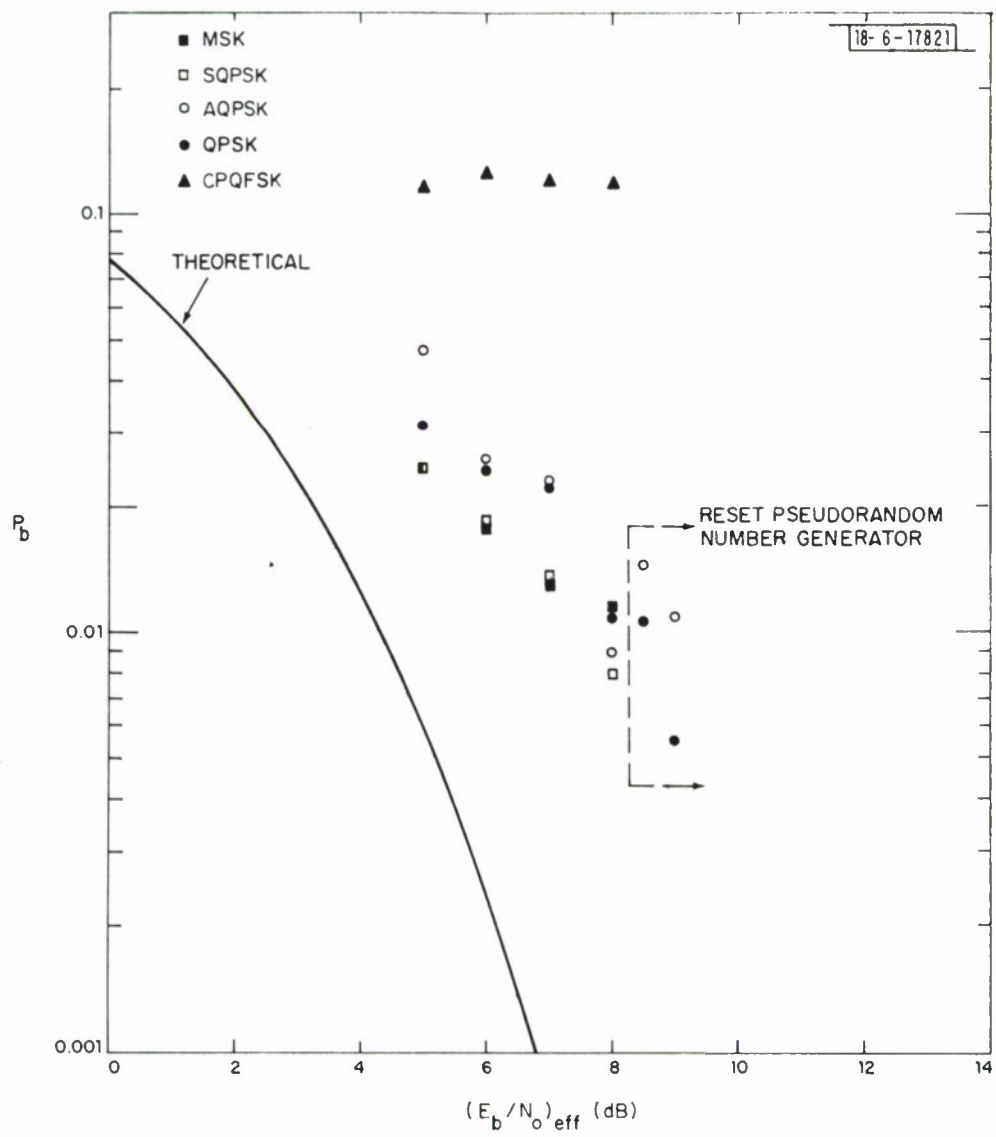b. Cubic phase, 36° deviation, 15.7/R delay.

Fig. 3.5. Continued.

c. Quadratic phase, 36° deviation, 15.7/R delay.

Fig. 3.5. Continued.

48

d. Cubic phase, 36° deviation, 15.2/R delay.

Fig. 3.5. Continued.

in Fig. 3.6. In view of the sharper roll-off of the FLEETSAT filter these losses are somewhat optimistic at the larger data rates (see Fig. 1.3a).

Most of the filter-6 simulation data can be condensed into Fig. 3.7 which gives the approximate degradation as a function of the data rate to filter 3-dB bandwidth ratio R/B. The high degradation portions of the BPSK and CPQFSK curves were based on loss data considerably above 4 dB.

Based on Fig. 3.7 the maximum feasible data rates for each modulation scheme are listed in Table 3.3. These estimates turned out to be somewhat optimistic when considering the greater selectivity of the FLEETSAT filter. But as before, we observe that MSK and SQPSK are the best modulations for the narrow bandlimited channel, followed by QPSK, AQPSK, CPQFSK and BPSK.
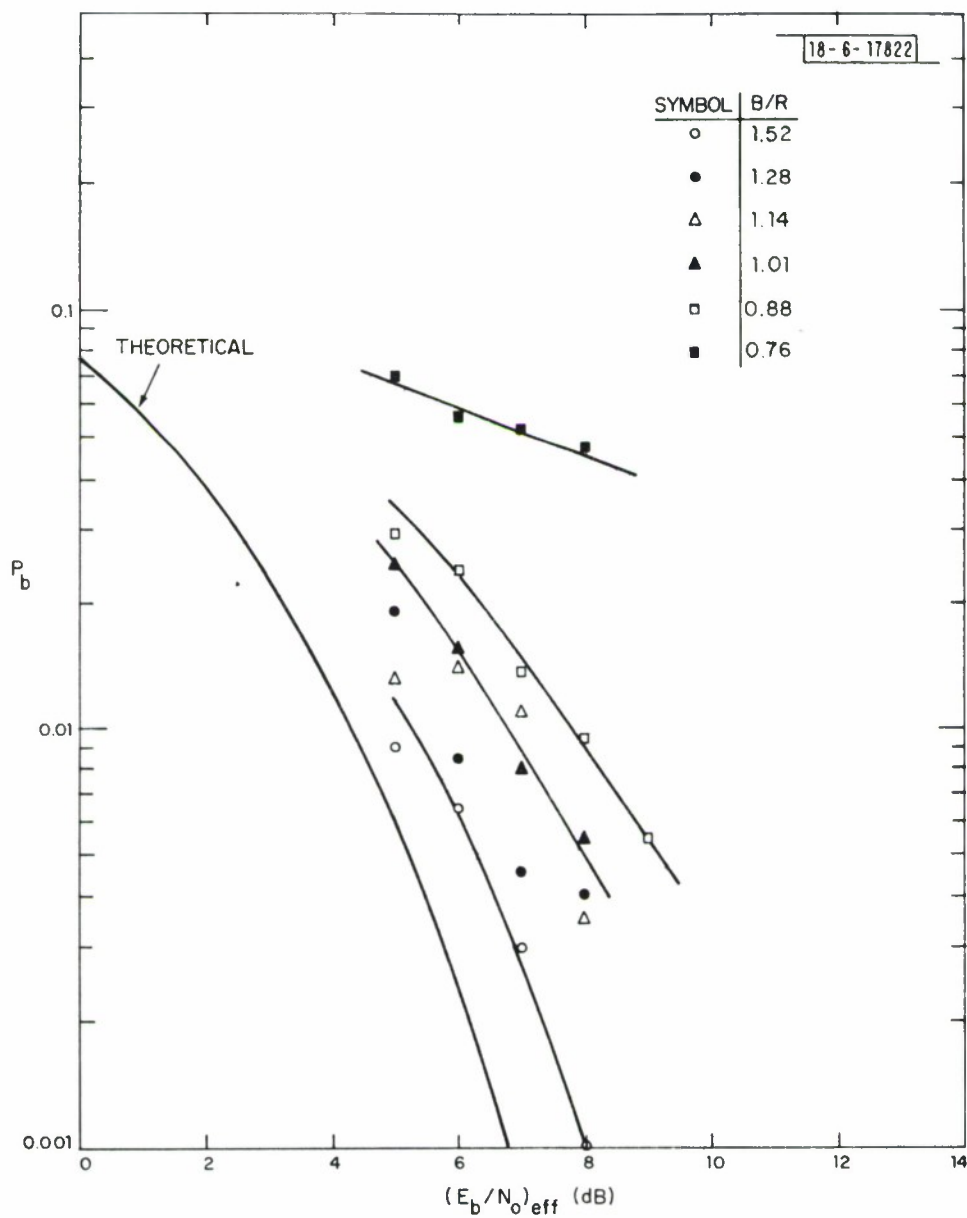
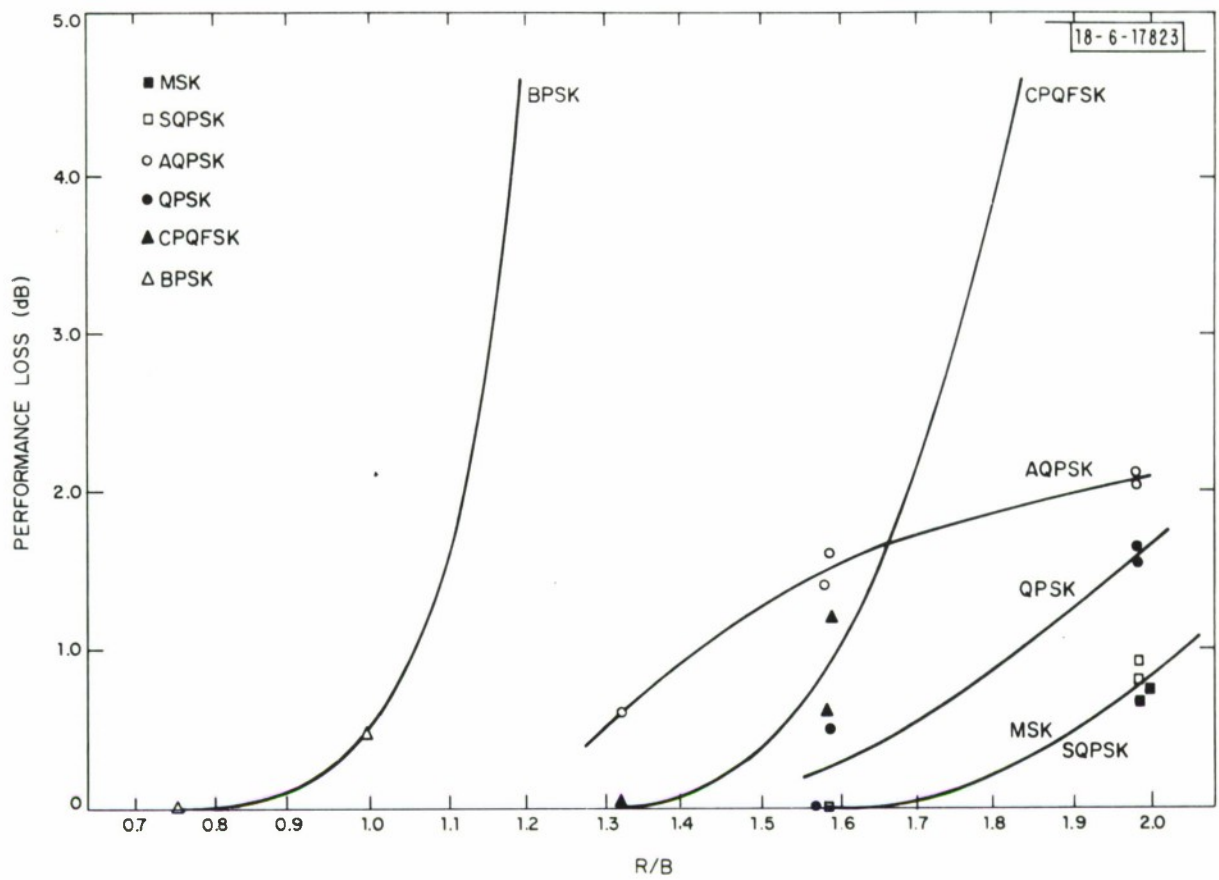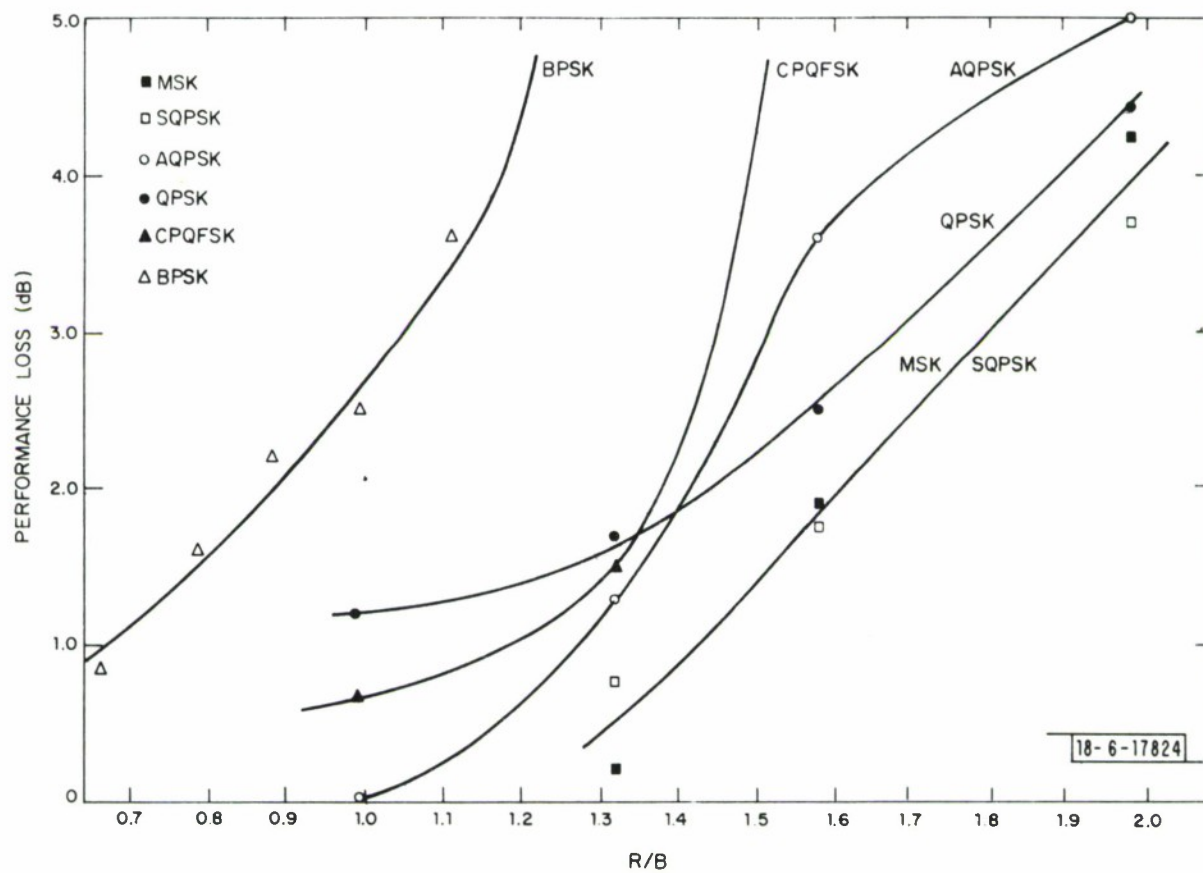Fig. 3.6. BPSK performance for cubic-phase filter, bandpass limiter, random data, and balanced links (36° deviation; 15.2/R delay).

51

a. 12° deviation, $15.7/R$ delay.

Fig. 3.7. Estimated degradation from theoretical at $P_b \approx 0.005$ vs. R/B for cubic-phase filter 6, bandpass limiter, random data, and balanced links.

b. 36° deviation, 15.2/R delay.

Fig. 3.7. Continued.

TABLE 3.3

ESTIMATED MAXIMUM FEASIBLE DATA RATES[*]
THROUGH THE 25-kHz SATELLITE MODEL WITH FILTER 6
FOR A 2-dB PERFORMANCE LOSS AT $P_b \approx 0.005$

Modulation	12°	Cubic Phase Deviation at 8.8 kHz from Band Center	36°
BPSK	28 kbps		20 kbps
MSK	56 kbps		40 kbps
SQPSK	56 kbps		40 kbps
AQPSK	48 kbps		36 kbps
QPSK	52 kbps		36 kbps
CPQFSK	44 kbps		32 kbps

[*] given to the nearest 4 kbps

54

APPENDIX A

Derivation of $(E_b/N_o)_{eff}$

Let B be the bandwidth, let P_{up} and P_{down} be the received signal power on the uplink and downlink, respectively, and let $(N_o)_{up}$ and $(N_o)_{down}$ be the corresponding single-sided AWGN power spectral densities. Suppose that we can ignore any ISI effects and that the ideal bandpass limiter alters the input SNR by a factor γ, i.e., suppose that the output SNR is

$$SNR_{out} = \gamma SNR_{in} = \frac{\gamma(P/N_o)_{up}}{B} \tag{A.1}$$

where we write $(P/N_o)_{up}$ for $P_{up}/(N_o)_{up}$. Then the fraction of received downlink signal power devoted to the uplink signal is $\gamma P_{up}/(\gamma P_{up} + (N_o)_{up}B)$ and the fraction devoted to uplink noise is $(N_o)_{up}B/(\gamma P_{up} + (N_o)_{up}B)$. The effective SNR at the receiver can be defined as the ratio of the received signal power devoted to uplink signal and the sum of the downlink noise power $(N_o)_{down}B$ and the received signal power devoted to uplink noise, i.e.,

$$SNR_{eff} = \frac{(P/N_o)_{eff}}{B} = \frac{(\frac{\gamma P_{up}}{\gamma P_{up} + (N_o)_{up}B})P_{down}}{(N_o)_{down}B + (\frac{(N_o)_{up}B}{\gamma P_{up} + (N_o)_{up}B})P_{down}}. \tag{A.2}$$

Since the power P can be generically expressed in terms of the energy per bit E_b and the data rate R as $P = E_b R$, we can rewrite (A.2) as

$$(E_b/N_o)_{eff} = \frac{\gamma (E_b/N_o)_{up} (E_b/N_o)_{down}}{\gamma (E_b/N_o)_{up} + \frac{B}{R} + (E_b/N_o)_{down}} . \tag{A.3}$$

Now (2.2) follows by setting the γ of (A.1) equal to unity in (A.3).

We now argue that $\gamma = 1$ results in a good approximation to the true E_b/N_o by considering the limiting cases of strong and weak links, where we take $E_b/N_o \gg 1$ for a strong link and $E_b/N_o \ll 1$ for a weak link. We further assume that $B/R \approx 1$.

Suppose first that the uplink is strong, i.e., $(E_b/N_o)_{up} \gg 1$. As mentioned in Section 2.1.2 this implies that $\gamma = 2$. If the downlink is weak, i.e., if $(E_b/N_o)_{down} \ll 1$, then (A.3) reduces to $(E_b/N_o)_{eff} \approx (E_b/N_o)_{down}$, independent of γ, which agrees exactly with our $\gamma = 1$ approximation (2.2) in this downlink noise limited case. If the downlink is strong, there are two subcases to consider. In the first subcase, $(E_b/N_o)_{up} \gg (E_b/N_o)_{down} \gg 1$, and again $(E_b/N_o)_{eff} \approx (E_b/N_o)_{down}$ from both (A.3) and (2.2); we are still downlink noise limited.

In the second subcase, $(E_b/N_o)_{down} \gg (E_b/N_o)_{up} \gg 1$, and $(E_b/N_o)_{eff} \approx \gamma (E_b/N_o)_{up} = 2(E_b/N_o)_{up}$. In this instance the model leading to (A.3) is faulty because the true effective E_b/N_o cannot exceed the (E_b/N_o) of the weakest link, i.e., the system is not Gaussian. This has been verified experimentally in Fig. 3.4c, for example. With $\gamma = 1$, our approximation (2.2) is okay if the ISI effects are not too great, or provided we process sufficiently at the receiver to mitigate the ISI.

$$(E_b/N_o)_{eff} = \frac{\gamma(E_b/N_o)_{up}(E_b/N_o)_{down}}{\gamma(E_b/N_o)_{up} + \frac{B}{R} + (E_b/N_o)_{down}} \quad . \tag{A.3}$$

Now (2.2) follows by setting the γ of (A.1) equal to unity in (A.3).

We now argue that $\gamma=1$ results in a good approximation to the true E_b/N_o by considering the limiting cases of strong and weak links, where we take $E_b/N_o \gg 1$ for a strong link and $E_b/N_o \ll 1$ for a weak link. We further assume that B/R 1.

Suppose first that the uplink is strong, i.e., $(E_b/N_o)_{up} \gg 1$. As mentioned in Section 2.1.2 this implies that $\gamma=2$. If the downlink is weak, i.e., if $(E_b/N_o)_{down} \ll 1$, then (A.3) reduces to $(E_b/N_o)_{eff} \approx (E_b/N_o)_{down}$, independent of γ, which agrees exactly with our $\gamma=1$ approximation (2.2) in this downlink noise limited case. If the downlink is strong, there are two subcases to consider. In the first subcase, $(E_b/N_o)_{up} \gg (E_b/N_o)_{down} \gg 1$, and again $(E_b/N_o)_{eff} \approx (E_b/N_o)_{down}$ from both (A.3) and (2.2); we are still downlink noise limited.

In the second subcase, $(E_b/N_o)_{down} \gg (E_b/N_o)_{up} \gg 1$, and $(E_b/N_o)_{eff} \approx \gamma(E_b/N_o)_{up} = 2(E_b/N_o)_{up}$. In this instance the model leading to (A.3) is faulty because the true effective E_b/N_o cannot exceed the (E_b/N_o) of the weakest link, the system is not Gaussian. This has been verified experimentally in Fig. 3.4c, for example. With $\gamma=1$, our approximation (2.2) is okay if the ISI effects are not too great, or provided we process sufficiently at the receiver to mitigate the ISI.

57

Now suppose that the uplink is weak so that $\gamma = \pi/4$ [18, p. 311, Prob. 13]. If the downlink is strong, (A.3) reduces to $(E_b/N_o)_{eff} \approx \gamma (E_b/N_o)_{up}$ which is only about 1 dB smaller than the $(E_b/N_o)_{up}$ obtained with $\gamma = 1$ from (2.2). Finally, if the downlink is weak, (A.3) reduces to $(E_b/N_o)_{eff} \approx (\gamma R/B)(E_b/N_o)_{up}(E_b/N_o)_{down}$, which again is about 1 dB smaller than the $\gamma = 1$ approximation.

APPENDIX B

Filter Characteristics

Some properties of the principal filters simulated are listed in Table B.1 using standard digital signal processing terminology [40]. We will provide the magnitude and phase responses for filters 1, 2, 4 and 6 and the impulse responses of filter 6 in this appendix. Frequency responses for filters 3 and 5 were reported in [37] and [39], respectively.

The Chebyshev and Butterworth filters were designed using [41] and realized in parallel canonical form, whereas the elliptic filter was obtained utilizing a readily available design program [42] and implemented in cascade canonical form. Hence, these causal, Infinite Impulse Response (IIR) filters were realized entirely in the time domain.

The computed responses for the IIR filters are shown in Figs. B.1 and B.2. The Chebyshev filter is equiripple in the passband, the Butterworth filter is maximally flat at f=0, and the elliptic filter is equiripple in both the passband and the stopband. These magnitude properties are preserved from the analog domain, thanks to a pre-warping of the critical analog frequencies and the use of the bilinear transformation during the design process [23, 24].

Using frequency sampling techniques, filters 3 and 6 were selected from [36] and filter 5 was modeled according to the FLEETSAT filter characteristics of Section 1.1. All three FIR filters were simulated nonrecursively by the overlap-add method [23, 24]. This involved sectioning the input sequence into equal segments, generally much shorter than the impulse response of the

TABLE B.1

DIGITAL FILTERS SIMULATED

Index	Type	Nominal Analysis Bandwidth (kHz)*	Phase	Number of Poles (IIR) or Nonzero Frequency Samples (FIR)	Maximum Sidelobe Level (dB)	Realization	Length of Impulse Response	Correlation Delay Used (sampling intervals)	Delay of Impulse Response Peak (sampling intervals)
1	IIR@ (Chebyshev)	481	nonlinear	8	$-\infty$	parallel (causal)	∞	45	49
2	IIR (Butterworth)	556	nonlinear	10	$-\infty$	parallel (causal)	∞	50	52
3	FIR+	109	linear	11	-62	nonrecuraive (non-cauaal)	32	0	0
4	IIR (elliptic)	207	nonlinear	10	-73	cascade (causal)	∞	16	17.5
5	FIR	1B5	nonlinear	128	-23	nonrecursive (causal)	64	31	31
6	FIR	198	cubic#12° 36°	13	-58 -36	nonrecursive (causal)	64	63 61	63 61

*Normalized to 3-dB bandwidth of 25 kHz.

+Finite Impulse Response

#The nominal phase deviation at 10 kHz from band center was either 12 or 36 degrees.

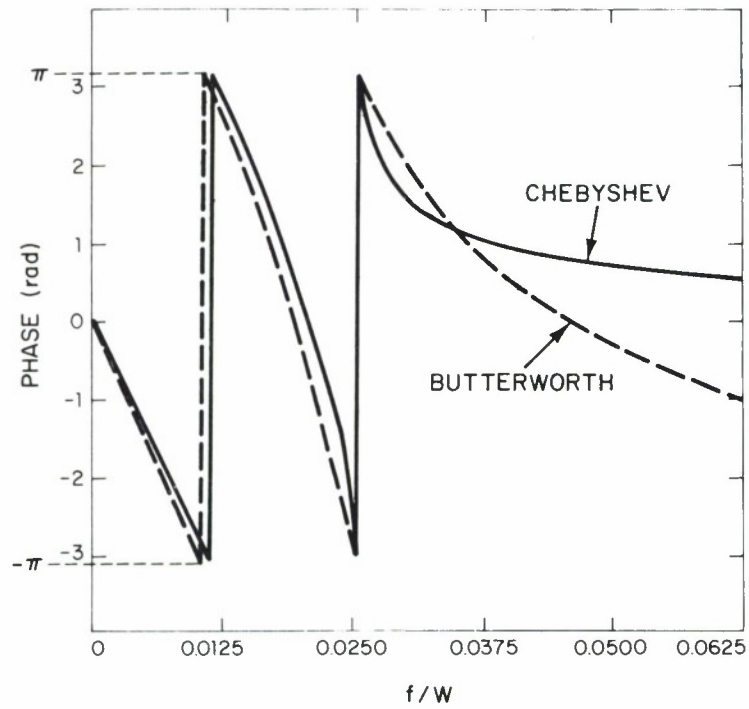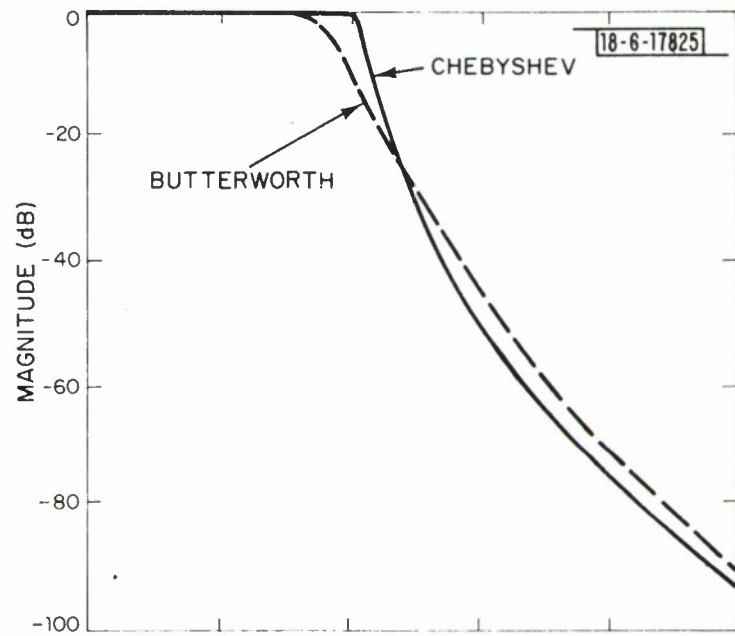@Infinite Impulse Response

60

Fig. B.1. Response of Chebyshev and Butterworth filters.
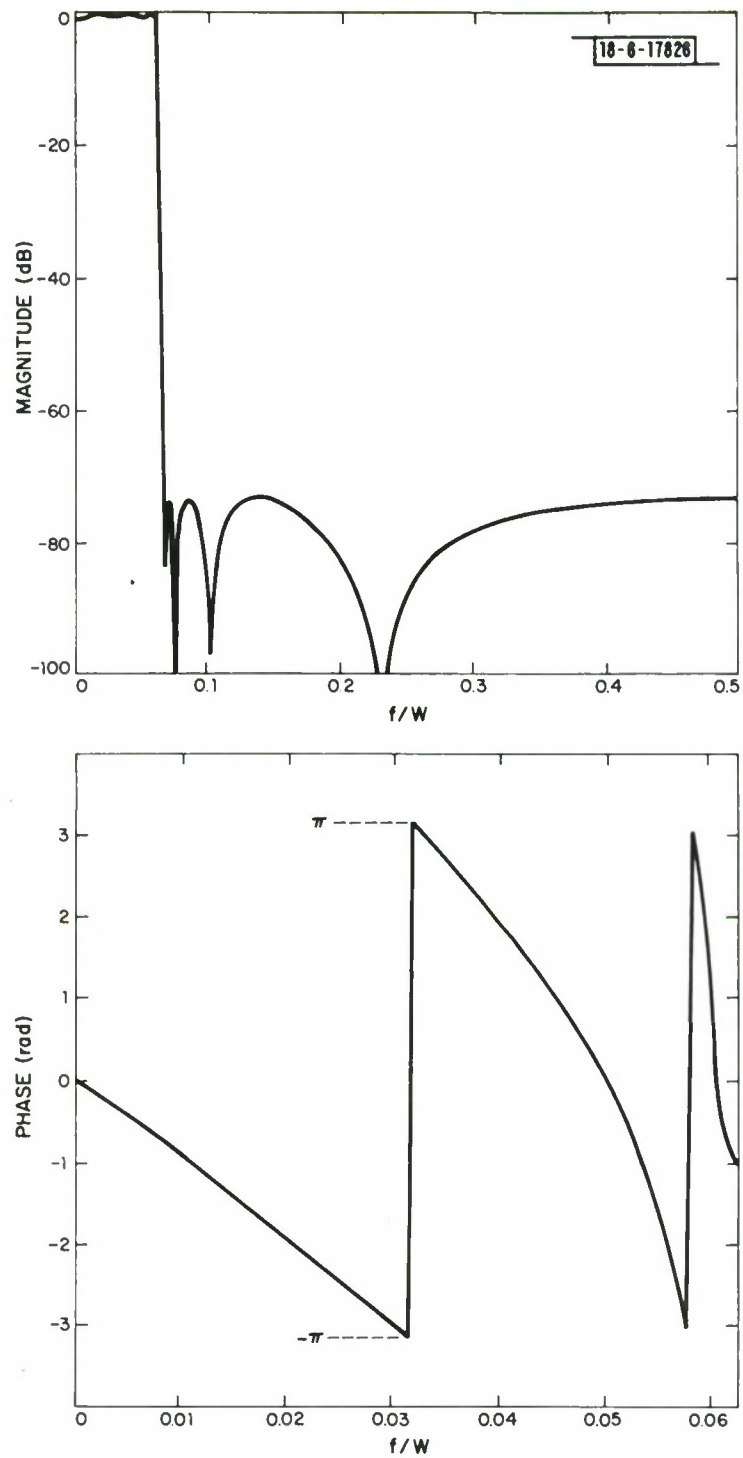
Fig. B.2.   Response of elliptic filter.

filter, padding with complex zeros at the end of each segment to twice the response length, and taking fast Fourier transforms (FFT's). Multiplying the frequency transforms of appropriately padded input and impulse response sequences corresponds to a convolution of the two finite length sequences. Naturally, the impulse response transform need be found only once.

Although every FIR filter can be realized with a frequency sampling structure in the time domain, they are usually implemented with the above fast convolution technique. However, a time domain realization can require fewer multiplications if nearly all the frequency samples are zero [43].

The impulse responses for all but filter 3 were non-anticipatory, i.e., causal. Valid results can be obtained by simulating non-causal filters, however, the only differences being in the output delay and programming convenience.

With filter 3 we padded in the middle of the impulse response since the linear-phase filter designs of [36] yield impulse responses in a non-causal form with the peak at the origin. Alternatively, we could have rotated the impulse response by half its length to obtain the causal form and then padded with an equal number of zeros on either side as we did with filter 6. We padded at the end of the impulse response with filter 5. In each case the number of complex zeros inserted equaled the impulse response length, which means the frequency response was interpolated to twice the number of original frequency samples.

A causal linear-phase FIR filter with a real impulse response has a phase delay of $(N-1)/2$ samples and an even impulse response, i.e., $h(N-1-n) = h(n)$, where $h(n)$ is the nth sample of a response of length N [24, p. 78]. The main worry with the nonlinear-phase FIR filters 5 and 6 is the fact that their impulse responses can be rather uneven, as we shall see for filter 6. We have verified that the responses for filters 5 and 6 have negligible imaginary parts, so one expects the peak of the causal impulse response to appear at about the $(N/2)$th sample, as in the linear-phase case.

For all filters simulated the correlation delay in seconds T_d is related to the number of samples in the delay N_d by

$$T_d = N_d/W \tag{A.1}$$

where W is the complex sampling rate.

The impulse and magnitude responses for the cubic-phase filter 6 are shown in Fig. B.3. The phase deviation from linearity in degrees was specified by $D(f/10^4)^3$, where D is either 12 or 36 degrees and where f is the frequency deviation. In superimposing this phase deviation on a causally rotated linear-phase design selected from [36], we see from Fig. B.3a that the impulse response has become asymmetrical about 63/2 and that the peak has shifted to the left for the 36-degree case, but only by 2 samples. These impulse responses were padded on each side with 32 zeros in obtaining the interpolated frequency response. The correlation delays of Table B.1 for filter 6 resulted from the sum of the 32 samples on the left and the location of the peaks in Fig. B.3a.

64
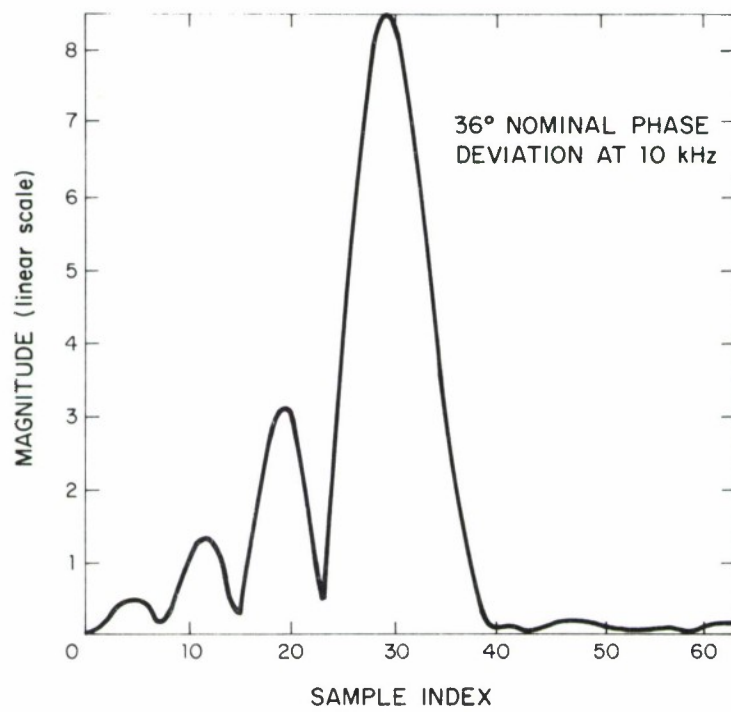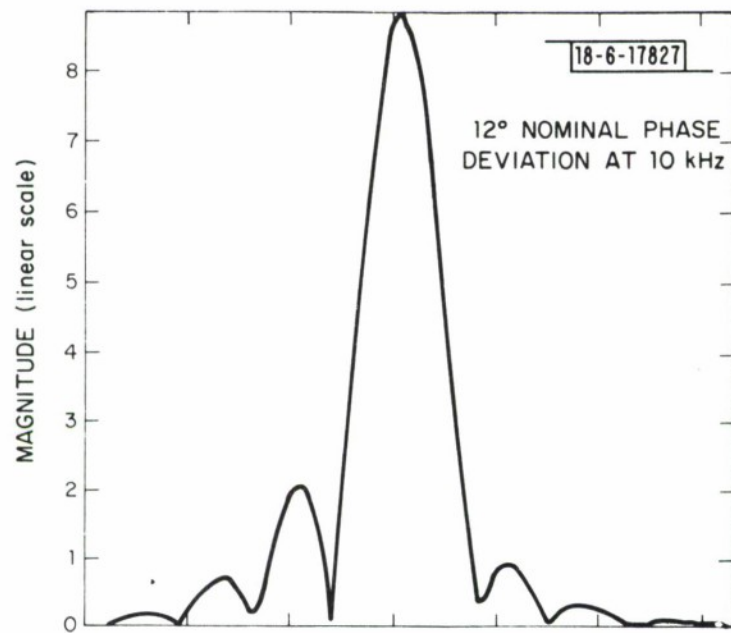
a. Impulse response.

Fig. B.3. Characteristics of cubic-phase FIR filter 6.
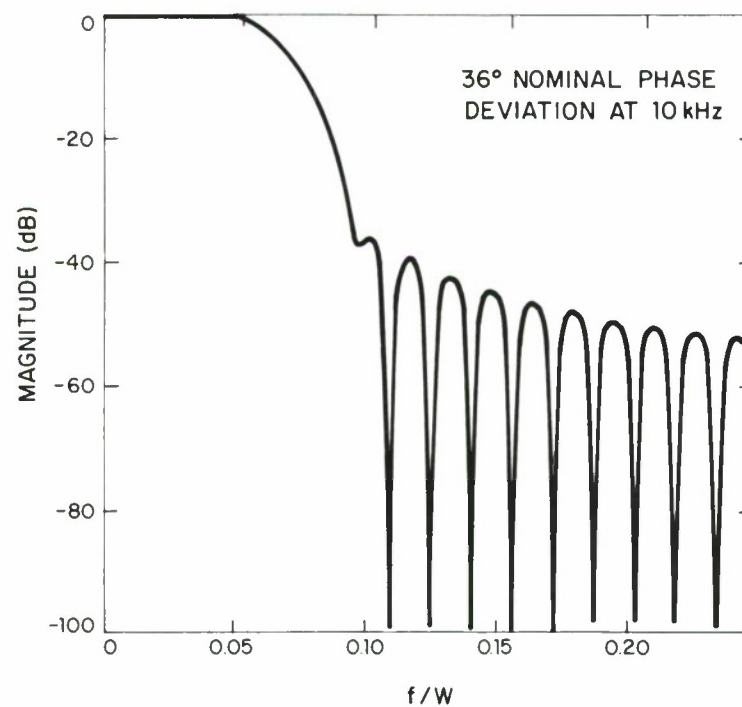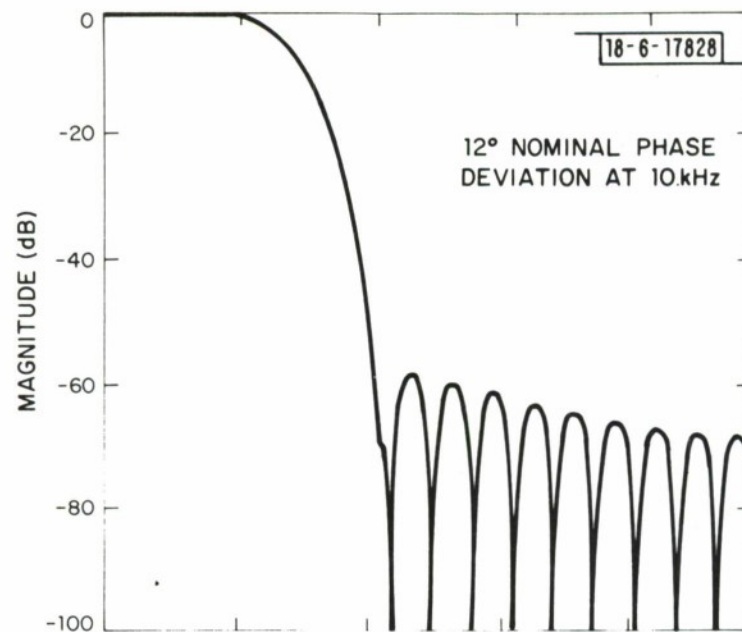
b. Frequency response.

Fig. B.3. Continued.

66

We verified that changing the sign of the cubic-phase deviation results in an impulse response that is essentially a reflection of the response of Fig. B.3a about a vertical line through its peak. In other words, the larger sidelobes appear after the main lobe, as with the IIR filter impulse responses which all had negative phase deviations (see Figs. B.1 and B.2). By this symmetry, the sign of the phase deviation should not affect the simulated results for filter 6.

A quadratic-phase version with the phase deviation of $sgn(f) \cdot D(f/10^4)^2$ was also simulated (see Fig. 3.5c). In this instance the maximum sidelobe level was -78 and -58 dB for $D=12^o$ and 36°, respectively (see Fig. B.3b). The asymmetry in the impulse responses for this quadratic case was less pronounced than in Fig. B.3a.

ACKNOWLEDGMENTS

REFERENCES

1. J. D. Bridwell and I. Richer, "A Preliminary Design of a TDMA System for FLEETSAT," Technical Note 1975-5, Lincoln Laboratory, M.I.T. (12 March 1975) DDC AD-A007823/8.

2. "Satellite Communications Set AN/WSC-3," Technical Manual, Operation and Maintenance Instructions, Naval Electronics Systems Command Report NAVELEX 0967-453-7010, Volume I, Electronic Communications, Inc., St. Petersburg, Florida (15 June 1973).

3. S. Lebowitz and L. Palmer, "Simulation Results for Intersymbol Interference Loss; QPSK Transmission Through Several Filter Types," Proc. 2nd IEEE National Telecommunications Conference, Atlanta, Georgia, 26-28 November 1973, pp. 32D-1 to 32D-7.

4. E. R. Wade, Electronic Communications, Inc., St. Petersburg, Florida, private communication.

5. H. R. Mathwich, J. F. Balcewica, and M. Hecht, "The Effects of Tandem Band and Amplitude Limiting on the E_b/N_0 Performance of Minimum (Frequency)Shift Keying (MSK)," IEEE Trans. Commun. COM-22, 1525-1540 (1974).

6. S. A. Gronemeyer and A. L. McBride, "Theory and Comparison of MSK and Offset QPSK Modulation Techniques Through a Satellite Channel," Proc. 4th IEEE National Telecommunications Conference, New Orleans, Louisiana, 1-3 December 1975, pp. 30-28 to 30-32; also see "MSK and Offset QPSK modulation," IEEE Trans. Commun. COM-24, 809-820 (1976).

7. J. J. Jones, "Filter Distortion and Intersymbol Interference Effects on PSK Signals," IEEE Trans. Commun. Technol. COM-19, 120-132 (1971).

8. E. Scheel, "Time Domain Analysis of Intersymbol Interference Effects on Phase Shift Keyed (PSK) and Quadrature Phase Shift Keyed (QPSK) Communication Systems," Proc. 9th IEEE Int. Conf. Commun., Seattle, Washington, 11-13 June 1973, pp. 14-21 to 14-26; also see "Phase Shift Keyed (PSK) and Quadrature Phase Shift Keyed (QPSK) Communication System Performance in Channels with Band-Limiting Filters," Proc. National Electronics Conference, Chicago, Illinois, 16-18 October 1974, pp. 310-315.

9. R. V. Groves and R. C. Beach, "Bandwidth Filtering Effects on PSK Modulation," Proc. IEEE National Aerospace and Electronics Conference, Dayton, Ohio, 13-15 May 1974, pp. 350-356.

10. V. K. Prabhu, "Optimum Bandwidth Occupancy in PSK Systems," Proc. 2nd IEEE National Telecommunications Conference, Atlanta, Georgia, 26-28 November 1973, pp. 24D-1 to 24D-3.

11. V. K. Prabhu, "Performance of Coherent Phase-Shift-Keyed Systems with Intersymbol Interference," IEEE Trans. Inform. Theory IT-17, 418-431 (1971).

12. H. C. Chan, D. P. Taylor, and S. S. Haykin, "Comparative Evaluation of Digital Modulation Techniques for Satellite Communications," Proc. IEEE Canadian Communications and Power Conference, Montreal, Canada, 7-8 November 1974, pp. 34-35.

13. J. M. Wozencraft and I. M. Jacobs, Principles of Communications Engineering (Wiley, New York, 1965).

14. R. E. Morley, Jr., "A Method of Combatting Intersymbol Interference in a Known Channel," not generally available.

15. G. D. Forney, Jr., "Maximum-Likelihood Sequence Estimation of Digital Sequences in the Presence of Intersymbol Interference," IEEE Trans. Inform. Theory IT-18, 363-378 (1972); also see 15a: Navy Communications Quarterly Technical Summary, Lincoln Laboratory, M.I.T. (15 January 1976), pp. 16-19, DDC AD-B010608-L.

16. H. B. Poza and H. L. Berger, "Performance Characterization of Advanced Wideband Data Links," Proc. 11th IEEE Int. Conf. Commun., San Francisco, California, 16-18 June 1975, pp. 4-23 to 4-27.

17. N. Morinaga, T. Mizuno, and T. Namekawa, "Transmission Characteristics of an M-ary Coherent PSK Signal via a Cascade of N Bandpass Hard Limiters-Application to Digital Satellite Communication Systems," Proc. 11th IEEE Int. Conf. Commun., San Francisco, California, 16-18 June 1975, pp. 35-26 to 35-30.

18. W. B. Davenport, Jr. and W. L. Root, An Introduction to the Theory of Random Signals and Noise (McGraw-Hill, New York, 1968).

19. J. G. Proakis, "Advances in Equalization for Intersymbol Interference," in Advances in Communication Systems Theory and Applications, Volume 4, A. J. Viterbi, Ed. (Academic Press, New York, 1975), pp. 123-198.

20. P. Hetrakul, D. P. Taylor, and S. S. Haykin, "Effect of a Soft-Limiter on the Error Rate of an M-ary CPSK System," Proc. 10th IEEE Int. Conf. Commun., Minneapolis, Minnesota, 17-19 June 1974, pp. 44B-1 to 44B-5.

21. P. C. Jain and N. M. Blachman, "Detection of a PSK Signal Transmitted Through a Hard-Limited Channel," IEEE Trans. Inform. Theory IT-19, 623-630 (1973).

22. M. F. Mesiya, P. J. McLane, and L. L. Campbell, "A Maximum Likelihood Receiver for Binary PSK Transmission Over a Bandlimited Nonlinear Channel," Proc. 4th IEEE National Telecommunications Conference, New Orleans, Louisiana, 1-3 December 1975, pp. 23-5 to 23-8.

23. A. V. Oppenheim and R. W. Schafer, Digital Signal Processing (Prentice-Hall, Englewood Cliffs, New Jersey, 1975).

24. L. R. Rabiner and B. Gold, Theory and Application of Digital Signal Processing (Prentice-Hall, Englewood Cliffs, New Jersey, 1975).

25. M. K. Simon, "On the Selection of a Sampling Filter Bandwidth for a Digital Data Detector," IEEE Trans. Commun. COM-20, 438-441 (1972).

26. A. Casini, G. Castellini, and P. Emiliani, "Sampling Rate Selection for a Digital Matched Filter," Proc. IEEE 63, 830-831 (1975).

27. B. E. White, "On the Close Packing of Unsynchronized FDM Waveforms," Technical Note 1975-34, Lincoln Laboratory, M.I.T. (14 October 1975), DDC AD-A021412; also, "A Worst-Case Crosstalk Comparison Among Several Modulation Schemes," submitted to IEEE Trans. Commun. (May 1976).

28. F. Chethik, "Analysis and Tests of Quadrature Advance/Retard Keying Modulation and Detection," Proc. 11th IEEE Int. Conf. Commun., San Francisco, California, 16-18 June 1975, pp. 21-21 to 21-25.

29. S. A. Rhodes, "Effects of Hardlimiting on Bandlimited Transmissions with Conventional and Offset QPSK Modulation," Proc. 1st IEEE National Telecommunications Conference, Houston, Texas, 4-6 December 1972, pp. 20F-1 to 20F-7.

30. V. K. Prabhu and H. E. Rowe, "Spectra of Digital Phase Modulation by Matrix Methods," Bell Syst. Tech. J. 53, 899-935 (1974).

31. B. E. White, "A Derivation of the Spectra of N-ary Orthogonal Continuous-Phase FSK Waveforms for ELF/VLF Communications," IEEE Trans. Commun. Technol. COM-19, 536-539 (1971).

32. R. R. Anderson and J. Salz, "Spectra of Digital FM," Bell Syst. Tech. J. 44, 1165-1189 (1965).

33. T. A. Schonhoff, "Bandwidth vs. Performance Considerations for CPFSK," Proc. 4th IEEE National Telecommunications Conference, New Orleans, Louisiana, 1-3 December 1975, pp. 38-1 to 38-5.

34. H. C. Peterson and E. W. Pike, "RAN2(K), A New Random Number Generator" and "RAN2(K) - Correction to S-0078;" also, "Addition to CMS User Guide", not generally available.

35. D. E. Knuth, Seminumerical Algorithms, The Art of Computer Programming, Vol. 2 (Addison Wesley, Reading, Massachusetts, 1969), pp. 104, 105.

36. L. R. Rabiner, B. Gold, and C. A. McGonegal, "An Approach to the Approximation Problem for Nonrecursive Digital Filters," IEEE Trans. Audio Electroacoust. AU-18, 83-106 (1970); also in Digital Signal Processing, L. R. Rabiner and C. M. Rader, Eds. (IEEE Press, New York, 1972), pp. 158-181.

37. Navy Communications Quarterly Technical Summary, Lincoln Laboratory, M.I.T. (15 July 1975), pp. 19-24, DDC AD-B007020-L.

38. R. E. Morley, Jr., Washington University, St. Louis, Missiouri, private communication.

39. Navy Communications Quarterly Technical Summary, Lincoln Laboratory, M.I.T. (15 October 1975), pp. 16-19, DDC AD-B008722-L.

40. L. R. Rabiner, J. W. Cooley, H. D. Helms, L. B. Jackson, J. F. Kaiser, C. M. Rader, R. W. Schafer, K. Steiglitz, and C. J. Weinstein, "Terminology in Digital Signal Processing," IEEE Trans. Audio Electroacoust. AU-20, 322-337 (1972); also in Literature in Digital Signal Processing, H. D. Helms and L. R. Rabiner (IEEE Press, New York, 1972), pp. 3-18.

41. R. Genesio, A. Laurentini, V. Mauro, and A. R. Meo, Butterworth and Chebyshev Digital Filters, Tables for Their Design (Elsevier, New York, 1973).

42. R. M. Mersereau, Georgia Institute of Technology, Atlanta, Georgia, private communication.

43. L. R. Rabiner, "Techniques for Designing Finite-Duration Impulse-Response Digital Filters," IEEE Trans. Commun. Technol. COM-19, 188-195 (1971); also in Digital Signal Processing, L. R. Rabiner and C. M. Rader, Eds. (IEEE Press, New York, 1972), pp. 150-157.

Abbreviations

AM	Amplitude Modulation
AQPSK	Alternating QPSK
AWGN	Additive White Gaussian Noise
BPSK	Binary Phase Shift Keying
CPBFSK	Continuous-Phase Binary Frequency Shift Keying
CPQFSK	Continuous-Phase QuadriFrequency Shift Keying
FFT	Fast Fourier Transform
FIR	Finite Impulse Response
FLEETSAT	unofficial designation for a military communications satellite
IIR	Infinite Impulse Response
ISI	InterSymbol Interference
MSK	Minimum Shift Keying
PM	Phase Modulation
QPSK	QuadriPhase Shift Keying
SNR	Signal-to-Noise Ratio
SQPSK	Staggered (offset) QPSK
TWT	Traveling Wave Tube
UHF	Ultra High Frequency
VHF	Very High Frequency
WSC-3	satellite communications set AN/WSC-3

Symbols

B	satellite filter 3-dB bandwidth
E_b	received signal energy per data bit
$(E_b/N_o)_{down}$	downlink E_b/N_o
$(E_b/N_o)_{eff}$	effective E_b/N_o
$(E_b/N_o)_{up}$	uplink E_b/N_o
f	frequency deviation
N_o	single-sided noise power spectral density
P_b	bit error probability
R	data rate
W	analysis bandwidth (complex sampling rate)

External Distribution List

The Defense Documentation Center
Attn: TISIA-1
Cameron Station, Bldg. 5
Alexandria, Virginia 22314 (2 copies)

Chief of Naval Operations (OP 941E)
Department of the Navy
Washington, D. C. 20350

Computer Sciences Corporation
Systems Division
6565 Arlington Blvd.
Falls Church, Virginia 22046
Attn: Mr. C. C. Ingram
Attn: Mr. J. Burgess .

Defense Communications Agency
8th and South Courthouse Road
Arlington, Virginia 22204
Attn: Dr. Frederick Bond
Attn: Dr. I. L. Lebow
Attn: Dr. P. Jain

Naval Electronics Laboratory Center
San Diego, California 92152
Attn: R. U. F. Hopkins, Code 2420
Attn: Library

U. S. Naval Underwater Systems Center
New London Laboratory
Ft. Trumbull
New London, Connecticut 06321
Attn: Mr. John Merrill

Naval Postgraduate School
Electrical Engineering Dept.
Monterey, California 93940
Attn: Prof. John Ohlson, Code 52
Attn: Library

Commander
Naval Electronics Systems Command
Department of the Navy
Washington, D. C. 20360
Attn: PME-117

NESC (continued)
Attn: PME-106
Attn: PME-106-1, Capt. J. Pope
Attn: PME-106-1, Lt. Cdr. J. Waylan
                              (6 copies)
Attn: PME-106-1, J. Nooney
Attn: ELEX-03, T. B. Hughes
Attn: ELEX-00B, Dr. J. Lawson

U. S. Naval Research Laboratory
4555 Overlook Avenue, S. W.
Washington, D. C.
Attn: Code 5370, Mr. G. Goodman
Attn: Code 5400
Attn: Code 5404, Dr. W. S. Ament
Attn: Code 5406, Cdr. N. L. Wardle
Attn: Code 5430, Mr. Leavitt
Attn: Code 5430, Dr. LeFande

Department of the Navy
Command Support Programs, OP-094H
Washington, D. C. 20350
Attn: Dr. R. Conley

Department of the Navy
Naval Telecommunication Division
OP-941T
4401 Massachusetts Avenue
Washington, D. C. 20350

Department of the Navy
Naval Telecommunication Systems
       Architect, OP-941N
4401 Massachusetts Avenue
Washington, D. C. 20350 (2 copies)
Attn: Dr. N. McAllister (1 copy)

Joint Tactical Communication Office
                              (TRI-TAC)
Code TT-E-EX
Fort Monmouth, New Jersey 07703
Attn: Lt. Col. Ralph Maruca, Jr.

Director, Telecommunication and Command
    & Control Systems (D/TACCS)
Pentagon, 3D-161
Washington, D. C.
Attn: Mr. G. Salton
Attn: Capt. R. Runyon
Attn: Dr. J. Neil Birch
Attn: Dr. J. Babcock

Institute for Defense Analysis
400 Army Navy Drive
Arlington, Virginia 22202
Attn: Dr. J. Aein

Rome Air Development Center
Griffiss Air Force Base
New York 13440
Attn: Mr. T. F. Treadway

Air Force Systems Command, XRTS
Andrews Air Force Base
Washington, D. C. 20331
Attn: Maj. J. Baker

Headquarters, U. S. Air Force, RDS
Pentagon Room 5D-320
Washington, D. C.

U. S. Army Satellite Comm. Agency
Fort Monmouth, New Jersey 07703
Attn: D. L. Labanca

The MITRE Corporation
Bedford, Mass. 01730
Attn: E. Crampton
Attn: W. T. Brandon

ESD/DCKS
Headquarters
L. G. Hanscom Field
Bedford, Mass. 01730
Attn: M. Chaskin

Mr. Robert L. Feik, Director
Operations Research Analysis
AFCS (CSMOA)
Scott Air Force Base, Illinois

Defense Communications Eng. Center
1860 Wiehle Avenue
Reston, Virginia 22090
Attn: G. E. LaVean

USAF-Avionics Laboratory
AFAL/AAI
WPAFB, Ohio
Attn: A. Johnson

Astro Electronics Division
RCA Corporation
Princeton, New Jersey 08540
Attn: H. R. Mathwich
Attn: J. T. Balcewicz
Attn: M. Hecht

Electronic Communications, Inc.
St. Petersburg, Florida 33733
Attn: E. R. Wade

Electrical Engineering Department
Washington University
Box 1127
St. Louis, Missouri 63130
Attn: R. E. Morley, Jr.

Collins Radio Group
Rockwell International Corp.
Dallas, Texas
Attn: S. A. Gronemeyer
Attn: A. L. McBride

Officer-in-Charge
U.S. Naval Shore Electronics
  Engineering Activity, Guam
Box 194
FPO San Francisco, Calif. 96630
Attn: Lt. Cdr. George Burman

REPORT DOCUMENTATION PAGE		READ INSTRUCTIONS BEFORE COMPLETING FORM
1. REPORT NUMBER ESD-TR-76-219	2. GOVT ACCESSION NO.	3. RECIPIENT'S CATALOG NUMBER
4. TITLE *(and Subtitle)* Simulation of a Narrow Bandpass-Limited Satellite Channel		5. TYPE OF REPORT & PERIOD COVERED Technical Note
		6. PERFORMING ORG. REPORT NUMBER Technical Note 1976-10
7. AUTHOR(s) Brian E. White		8. CONTRACT OR GRANT NUMBER(s) F19628-76-C-0002
9. PERFORMING ORGANIZATION NAME AND ADDRESS Lincoln Laboratory, M.I.T. P.O. Box 73 Lexington, MA 02173		10. PROGRAM ELEMENT, PROJECT, TASK AREA & WORK UNIT NUMBERS Program Element No. 33109N
11. CONTROLLING OFFICE NAME AND ADDRESS Naval Electronic Systems Command Department of the Navy Washington, DC 20360		12. REPORT DATE 28 July 1976
		13. NUMBER OF PAGES 84
14. MONITORING AGENCY NAME & ADDRESS *(if different from Controlling Office)* Electronic Systems Division Hanscom AFB Bedford, MA 01731		15. SECURITY CLASS. *(of this report)* Unclassified
		15a. DECLASSIFICATION DOWNGRADING SCHEDULE

16. DISTRIBUTION STATEMENT *(of this Report)*

Approved for public release; distribution unlimited.

17. DISTRIBUTION STATEMENT *(of the abstract entered in Block 20, if different from Report)*

18. SUPPLEMENTARY NOTES

None

19. KEY WORDS *(Continue on reverse side if necessary and identify by block number)*

Navy communications   modulation techniques
FLEETSAT   satellite communications

20. ABSTRACT *(Continue on reverse side if necessary and identify by block number)*

The effects of a bandpass-limiting satellite channel, such as a B=25-kHz hard-limiting FLEETSAT channel, on several modulation techniques were simulated. The modulations included BPSK and various forms of QPSK, including offset QPSK and continuous-phase minimum frequency shift keying (MSK). Coherent matched-filter receivers and both uplink and downlink noise were assumed.

For a bit error probability of 0.005 and a SNR loss of less than 1 dB caused by the nonlinearity in the FLEETSAT case, the maximum standard data rate R was 19.2 kbps for BPSK but 32 kbps for offset QPSK, MSK and QPSK. Rates of 24 kbps for BPSK and 48 kbps for offset QPSK and MSK were attainable at this same reliability with a SNR degradation of about 4 dB and 2.5 dB, respectively. Larger degradations are expected at lower error rates.